TARGET IMAGING FOR SFCW BASED TWI SYSTEM

A DISSERTATION

Submitted in partial fulfillment of the
requirements for the award of the degree
of
INTEGRATED DUAL DEGREE
(Bachelor of Technology & Master of Technology)
in
ELECTRONICS AND COMMUNICATION ENGINEERING
(With Specialization in Wireless Communication)

By

SANDEEP KUMAR

DEPARTMENT OF ELECTRONICS AND COMPUTER ENGINEERING
INDIAN INSTITUTE OF TECHNOLOGY ROORKEE
ROORKEE - 247 667 (INDIA)

JUNE, 2012

Candidate's Declaration

I hereby declare that the work, which is presented in this dissertation report entitled, **"TARGET IMAGING FOR SFCW BASED TWI SYSTEM"** towards the partial fulfilment of the requirements for the award of the degree of **Integrated Dual Degree (Bachelor of Technology and Master of Technology)** in Electronics and Communication Engineering with Specialization in **Wireless Communication,** submitted in the Department of Electronics and Computer Engineering, Indian Institute of Technology Roorkee, Roorkee (India) is an authentic record of my own work carried out during the period from June 2011 to June 2012, under the guidance of **Dr. Dharmendra Singh, Associate Professor, Department of Electronics and Computer Engineering, Indian Institute of Technology Roorkee.**

I have not submitted the matter embodied in this dissertation for the award of any other Degree or Diploma.

Date: 8 JUNE, 2012

Place: Roorkee

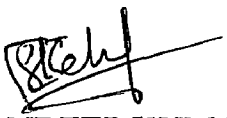

SANDEEP KUMAR

CERTIFICATE

This is to certify that the above statement made by the candidate is correct to the best of my knowledge and belief.

Date: 8 JUNE, 2012

Place: Roorkee

Dr. Dharmendra Singh

Associate Professor

E&C Department

IIT Roorkee

ACKNOWLEDGEMENT

On completion of the dissertation I want to thank everyone who helped me in direct or indirect way.

First of all, I would like to thank my dissertation guide, Dr. Dharmendra Singh for his constant guidance and motivation. His caring and encouraging attitude towards me was a big boon. He always managed to spare time for his students' research problems despite his extremely busy schedule. I still remember late hour meetings and discussions with him.

There are no words for appraisal of Remote Sensing Laboratory of the department for providing me such a great and healthy research environment. I am very thankful to its members Pooja Mishra, Tasneem Ahmed, Dharamveer Singh, Abhishek Singh, Shivangi Goel for giving me support in tough times and joy during light moments. I am grateful to my colleagues and RSL members Ghanshyam and Shailesh for listening to my ideas and giving me valuable suggestions. Special thanks to Dr. Rishi Prakash, Dr. A.N. Gaikwad, Mr. Prashant Chaturvedi, Mr. Shashikant Pandey to help me understand rudiments of this project.

I would also like to thank the faculty of the E&C department who laid strong base of RF & Microwave concepts for me. I am also thankful to Mr. Gore, Wireless Lab assistant for making sure the availability of equipments every time for conduction of experiment. I would like to appreciate help, suggestions and assistance offered to me by Mr. Akhilendra Singh, IIIT Gwalior student; for performing hours long tiresome experiments. A special thanks to Shrawan for his assistance and voluntarily acting as target for human related experiment.

I would like to thank my peer group especially E&CE IDD friends for providing me cool, tension free, light and healthy competitive environment. Without light and fun moments shared with them, this research work could be very stressful.

In the end I would like to express my gratitude towards my parents for their blessing, encouragement and my sisters for their moral support.

ABSTRACT

This work deals with the use of Stepped Frequency Continuous Wave (SFCW) radar in the frequency range of 1 GHz- 3GHz for Through Wall Imaging (TWI) applications. There are many challenges associated with Through Wall Imaging. Since the through wall applications are such that the capability of the system to perform in real time is important, PC is interfaced with the Vector Network Analyzer (VNA) and data acquisition and processing is carried out in real time. Detection of oriented targets is a big challenge for through wall imaging applications as oriented targets (especially metallic) reflects a major part of incident radiation away from transmitter antenna. So this detection has to be performed by using antenna in bistatic mode. Real time moving target detection is one of the prime areas in the field of through wall imaging as identifying moving objects and humans is the topmost priority. In this project detection of target with surface parallel to wall and moving perpendicular to wall is carried out. A metallic target was designed which acted as a human mock up and good results have been obtained by this mock target, but detection of a human target behind the wall is still a great challenge due to its complex dielectric properties and irregular shape resulting in uneven scattering. However with the help of ICA algorithm the detection of low dielectric substance is possible. The micro-Doppler characteristic of human body can be detected by SFCW radar at much lower sampling rates and power. With the help of high bandwidth of our present TWI system the moving activity like heart beat detection is possible. By technique named Range Doppler Processing the heart beat of a human at different standoff distances ranging 30 cm to 1 m was measured with small error.

ACRONYMS

2D	Two Dimensional
3D	Three Dimensional
CPI	Coherent Processing Interval
FCC	Federal Communications Commission
FFT	Fast Fourier Transform
HPBW	Half Power Band Width
ICA	Independent Component Analysis
IFFT	Inverse Fast Fourier Transform
RADAR	Radio Detection And Ranging
RF	Radio Frequency
SAR	Synthetic Aperture Radar
SFCW	Stepped Frequency Continuous Wave
SVD	Singular Value Decomposition
TWI	Through Wall Imaging
VNA	Vector Network Analyzer
UWB	Ultra Wide Band
MTI	Moving Target Indicator

CONTENTS

LIST OF FIGURES

Chapter 1

Introduction

Through-the-Wall Radar Imaging is an emerging technology, allowing to "see" through visually opaque material such as walls. It has numerous civilian, law enforcement and military applications making it a highly desirable tool in, for example, police and firefighter missions or search and rescue operations [1]. It allows police units to detect and locate hostages, hostage-takers and weapons in a hostage crisis before even entering the building and allows detecting and classifying concealed weapons and explosives in military actions or for security purposes. In all these applications, it is the ultimate aim to use radio frequency (RF) emission and reception to gain vision into scenes which otherwise are no accessible physically, optically, acoustically, or thermally [2].

One of the major challenges is to develop real time through wall imaging systems which can work in a variety of RF environments and walls. SFCW based RADAR is widely used for TWI applications because of lower signal distortions, high dynamic range, low power consumption and high signal to clutter ratio. Oriented targets i.e. the targets making certain angle with plane of wall need to be detected using antenna in bistatic mode, as earlier; the shape detected by antenna in monostatic was distorted. Movement detection of the targets behind the wall is the recent area of research in TWI. Extensive research is going on for detection of human and its metabolic activities like heart beat and breathing. Most of these methods identify the movement of heart and thorax by using the range resolution provided by UWB pulse radar systems. However, Range Doppler based on SFCW radar is capable of providing information about both frequency and distance of heart beat from antenna. There is a considerable amount of scope for research work aiming at improvements. To meet the challenges, research in TWI is directed mainly in areas of signal processing, pattern analysis techniques, antennas and electromagnetic related issues.

1.1. Motivation & Objective

Through wall imaging (TWI) is attracting more attention from various researchers because of its use in several civilian as well as in military applications. It is one of the most rapidly emerging technologies in which aim is to 'see' through visually opaque obstacles like different types of walls and detect as well as image various targets present behind the wall. Ultrasound, millimeter wave radiometry, infrared, and X-rays can be used for through wall imaging but RADAR sensor is the most suitable due the following reasons. Ultrasound technique can be used to detect and locate target behind metallic or nonmetallic wall but cannot be used for imaging due to high resolution requirement in TWI. Millimeter wave radiometer uses energies radiated by bodies of targets for detection but limitation is that it works only up to very short distances [3]. Infrared can be used to image target through wall at very short distance as attenuation through wall is very high. X-ray based sensors provide good imaging quality but are limited due to being expensive and medically unsafe.

The commonly employed RADAR systems for TWI application are impulse radar, Frequency Modulation Continuous Wave (FMCW) and Stepped Frequency Continuous Wave (SFCW) and noise radar. SFCW radar works in frequency domain where the frequency of each signal in the waveform is linearly increased in discrete steps, by a fixed frequency whereas impulse radar works in time domain transmitting a short time pulse and receives the backscattered signal by using either sampling receiver or extremely fast analog to digital converters. The idea of using SFCW [4, 5] radar is not new but due to its simple design and relatively lower cost, pulse radar dominated the industry. However the cost of microwave components has decreased considerably making it viable to design SFCW based radar system. SFCW radar system possesses several advantages over impulse type of radar systems which will be discussed in section 1.4.2 of the report. In a real situation, multiple targets or other objects will be present in general. Reflection due to unwanted objects and other sources contribute towards clutter which makes target detection in through wall imaging a difficult task. Work has been done on real time tracking the moving targets behind the wall in real time. Good results are expected for detecting targets moving normal to wall surface. In presence of human-mockup target there is a fair chance of false detection of human detection. However, the micro-Doppler characteristic of human body can be detected by SFCW radar at much lower sampling rates and power as frequency response

corresponding to metal target is different from that of human. It can help in distinguishing a living and a non-living target [6]. In nutshell, considerable amount of attention and research is required for dealing different problems of TWI systems. This motivated to develop processing techniques to improve detection, localization and recognition of the targets.

Keeping challenges and the needs in mind, following outline has been drawn for the present work.

- Comparative study of the response obtained for oriented targets for antenna operation in monostatic mode and bistatic mode.
- Real time detection of the targets moving normal to the wall using iterative time-domain response methodology.
- Detection and differentiation between human and dummy human metallic targets and their pattern analysis.
- Heart beat detection of human using Range- Doppler processing technique.

1.2 Types of Through Wall Imaging (TWI) System

Ferris and Currie [1] had carried out a survey of technologies applicable for through the wall surveillance. The technologies used for through wall imaging are classified as active or passive imaging. In active imaging, RF, acoustic, optical or X ray energy are used to estimate the reflectivity distribution of a remote scene and in passive imaging millimeter wave imaging radiometer are used which uses energies that is radiated by the bodies of persons within a building for detection [1].

Table 1.Technologies Applicable to Through Wall Surveillance [1]

Technology Area	Frequency Bands	Specific Application
Radio Frequency	VHF/UHF	Impulse Radar
	VHF/UHF	FMCW Radar
	Microwaves	Breathing Detection Radar
	Millimeterwaves	Heart Beat Detection Radar
		Imaging Radiometer
Acoustic	Sonic/Ultrasonic	Impulse Radar
X-Ray Scanner	X-Ray	Active Reflective /Transmissive Imager

Table 1 summarizes the commonly used technologies that provide a solution at some level to the through wall imaging problem. The advantages and disadvantages of above mentioned technologies are mentioned in section 1.1. The Stepped Frequency Continuous Wave (SFCW) radar was not included in the Table 1. Stepped Frequency Continuous Wave radar and short pulse radar represent two different techniques that are used currently to generate wide band of frequencies to detect hidden targets. Stepped frequency radar is frequency domain system whereas pulse radar is time domain system. SFCW radar system possesses several advantages over time domain systems. [8, 9] These will be discussed in sub section 1.4.2.

1.3. Ultra Wide Band Concept

Federal Communication Commission (FCC) [13] defined that, UWB signal has a relative bandwidth (bandwidth divided by center frequency) not smaller than 0.25 or a bandwidth not smaller than 500 MHz at any time during transmission [10].

$$B_{relative} = 2\frac{f_h - f_l}{f_h + f_l} = \frac{W}{f_c} \tag{1.1}$$

For UWB applications any waveform that satisfies the definition of UWB signal can be used as an excitation pulse. To achieve high resolution, high bandwidth is required. Conventional narrowband signals must use higher carrier frequency in order to achieve higher bandwidth. But as frequency increases, propagation loss through wall increases as shown in Fig 1.1. On the other hand, UWB signals can achieve high resolution with lower center frequency.

From eq. 1.1

$$fc = \frac{\omega}{B_{rel}} \tag{1.2}$$

$$f_{c1} < f_{c2} \text{ for } B_{rel1} > B_{rel2}$$

It shows that UWB signals have the capability for greater penetration of obstacles such as walls than do conventional signals while achieving same resolution. Hence, they are effective in dealing with power-bandwidth tradeoff.

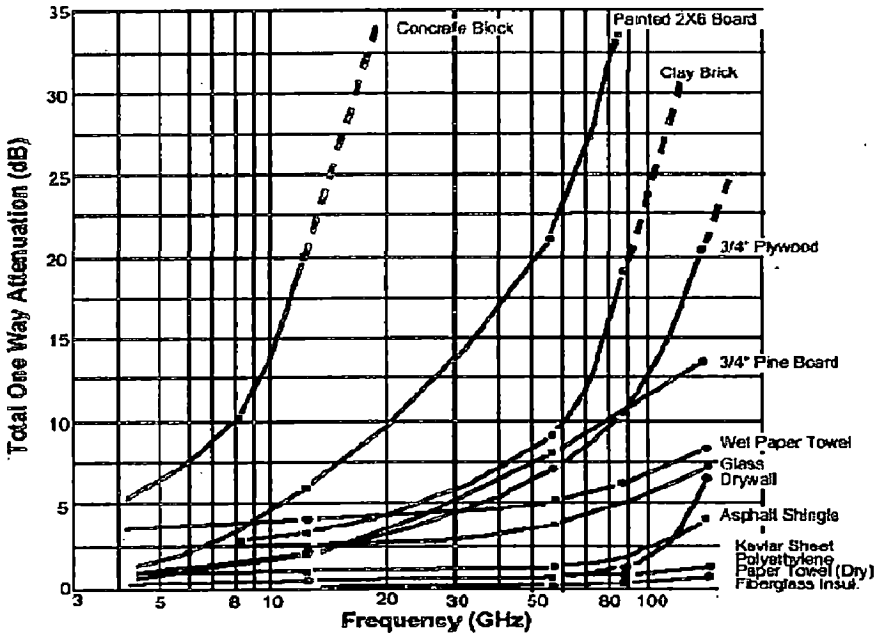

Figure 1.1 Attenuation through different types of walls [37]

Some of the advantages of UWB for through wall imaging applications are stated as following [7]:

1. Improved measurement accuracy of target range.
2. Identification of target class and type because a received signal carries the information not only about the target as a whole but also about its separate elements.
3. Decrease in radar dead zone.
4. Concealed radar operation due to radiation of signals which will be hard to detect.
5. It possesses good immunity against multipath interference, which is very strong within buildings.
6. Good resolving power due to which multiple targets can be resolved.

1.4. TWI system based on SFCW Radar and its parameters:

1.4.1. SFCW basics:

A frequency-domain pulse synthesis method, SFCW (Stepped-Frequency Continuous-Wave) is a widely used for radar systems. The SFCW radar operation is from a low frequency limit to a high frequency limit and the digital radio technology is used to provide this stepping up. Frequency is

increased in linear steps after fixed interval of time and this is commonly called frequency sweep. A step-frequency waveform can be viewed as an inter pulse modulated pulse compression waveform in which modulation is applied across the pulses rather than within individual pulses. [10]

By measuring the coherent target reflections over a number of stepped frequencies within the given bandwidth, these reflections are used to obtain distance for SFCW radar. This raw frequency data is then applied with IDFT to yield the scattering from individual targets. The waveform for step-frequency radar consists of a group of N coherent pulses with a constant frequency increment of Δf as shown in Figure 1.2. The frequency of nth pulse can be written as:

$$f_n = f_0 + n\Delta f \tag{1.3}$$

Where fo is starting carrier frequency and Δf is frequency step size N is the number of steps. Each pulse is τ seconds wide, and the time interval T between the pulses is adjusted for ambiguous or unambiguous range. The value of frequency is same within each pulse. A burst or Groups of N pulses are transmitted and received before any processing is initiated to realize the high-resolution potential of this waveform. The burst time, i.e., the time corresponding to transmission of N pulses will be called the coherent processing interval (CPI) as in conventional radars. Since the frequency is constant within the individual pulse, its bandwidth is approximately equal to the inverse of pulse width [38]. Pulses of typical time duration have narrow bandwidth, thus making the instantaneous bandwidth of the radar narrow.

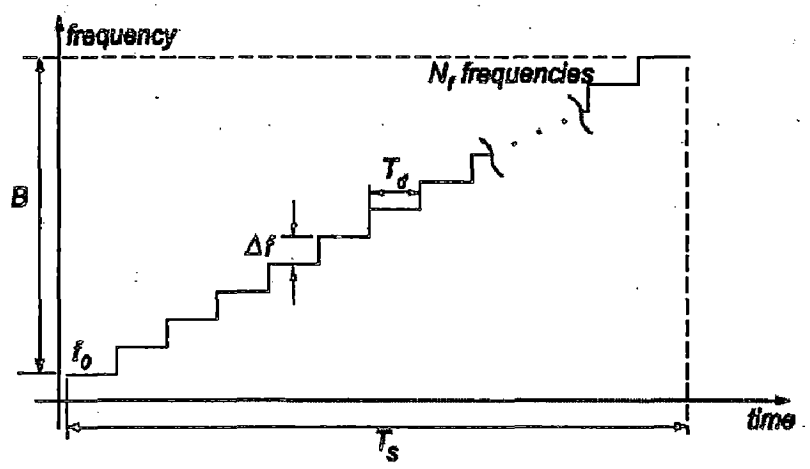

Figure 1.2: Stepped-frequency CW waveform with Nf frequencies [38].

SFCW radar determines distance information from the phase shift in a target reflected signal.. However, effective large bandwidth can be realized by appropriately processing the N pulses in a CPI. The effective bandwidth is determined by the total frequency excursion, i.e., $N\Delta f$ over the duration of N pulses.

The SFCW radar parameters for TWI application should be chosen carefully. The main parameters are number of frequency points and unambiguous range.

(a). Number of frequency points

SFCW radar illuminates target with consecutive train of number of frequencies and processes it coherently after receiving them. Thus the process gain will be high, if numbers of frequency points are high. The choice of high frequency points result in small frequency step size for better resolution. If the numbers of points are chosen smaller then data acquisition time is reduced.

(b). Unambiguous range

The unambiguous range that is maximum range in which target without ambiguity can be detected is given by

$$R_u = \frac{c}{2\Delta f} \tag{1.6}$$

From equation (1.6) if the frequency step is narrow then ambiguous range will be greater. For a given bandwidth if frequency points are more unambiguous range will be large but on contrary the processing time increases.

1.4.2 Advantages of SFCW based systems:

- The main advantage of the stepped frequency technique is that it covers wide bandwidth with lower signal distortions due to narrow instantaneous bandwidth.
- The other advantage of SFCW over impulse is greater measurement accuracy because it is much easier to synthesize a pure tone at a frequency than to measure a time delay i.e., accuracy with which the frequencies are set in SFCW radar is much greater than measurement time used in impulse radar [14]
- This technique is relatively easy with current technologies to efficiently sample ultra wideband signals with low speed analog to digital converters.

- SFCW has greater dynamic range and lower noise because it can transmit at higher power and uses a very narrow IF bandwidth.
- Calibration procedure removes many sources of time varying measurement error. Shaping of pulse is also possible with help of windowing for reducing side lobes.
- Measuring an object reflectivity in the frequency domain and applying an inversion technique to obtain the time history of physical space removes the requirements for wide instantaneous bandwidth and high sampling rate, leading to reductions in physical size, weight, complexity and cost of the radar hardware. [15]
- The other advantages are high dynamic range, low power consumption and high signal to clutter ratio. [9]

The drawback of SFCW radar is its long data acquisition time. But for a particular application like detection and imaging of stationary targets long data acquisition time is generally in acceptable range.

1.4.3. SFCW radar parameters:

(a) Range resolution:

Downrange resolution or range resolution is the capacity of the radar to discriminate individual elements that are close in down range as shown in Figure 1.3 (a). High downrange resolution for SFCW systems [9] is obtained by using wide bandwidth and is given as equation (1.5)

$$\Delta z = \frac{c}{2N\Delta f} \tag{1.5}$$

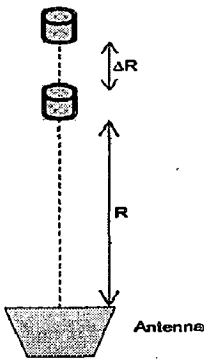

Figure 1.3 (a) Range resolution

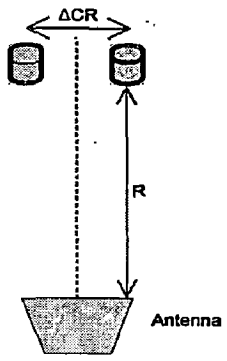

(b) Crossrange Resolution [34]

Where K is number of frequency points and Δf is step size. The required bandwidth must be greater than 1 GHz to obtain range resolution in order to detect object size of few centimeters. The actual value is taken more than theoretical value.

(b) Crossrange resolution:

Crossrange resolution is the capacity of the radar to discriminate individual elements that are close to each other in cross range as shown in Figure 1.3(b). Crossrange resolution is a function of wavelength at the lowest operating frequency, the length of physical antenna aperture and distance from antenna to target. For an antenna i^{th} aperture D, operating at wavelength the cross range resolution is defined as

$$CR \approx \frac{\lambda}{D} R \tag{1.6}$$

Where R is the range to target, λ is wavelength, D is physical aperture. For a real antenna, resolution degrades with increasing target distance.

For the narrow antenna beam width, line of sight signal can be easily picked, i.e., resolution enhancement with a narrower beam width. There are two methods to increase crossrange information content. One is by increasing the real aperture of the antenna, which is quite physically unmanageable. Another is synthetic aperture method, in which antenna moves point to point within predefined array. Processing the data allows us to synthesize an effective aperture many times the size of a real aperture [16]. If fixed array is used scanning time is reduced with increase in complexity of processing signals.

High frequency range is chosen to achieve narrow beam width of antenna. Thus high cross range resolution requires selection of higher frequency. But at high frequencies, penetration through the wall is low. Thus there is inherent tradeoff between resolution and penetration as already shown in Figure 1.1. In brick wall, one way attenuation is reported as 5 dB/cm at 5 GHz and in concrete it is 10 dB/cm at 3 GHz [17]. Better resolution and penetration are the major challenges being faced in TWI [34].

(c) Maximum target extent:

The maximum extent of the target should be less than the unambiguous range to avoid aliasing,. [9]

$$L_t < z_{\max} \tag{1.7}$$

For good delectability, the pulse width should be large enough to encompass the entire target length

$$L_t \leq c\tau/2 \tag{1.8}$$

where τ being the step duration of a single frequency in SFCW sweep.

1.5 System parameters selection

- Keeping in view the above discussion, a frequency range of 1 GHz- 3 GHz was chosen. The range is close to UWB and hence it offers the advantages as discussed in section 1.3.
- The bandwidth chosen is 2 GHz and the number of frequency points chosen for SFCW system is 201. This offers us a range resolution of 7.5 cm in accordance with equation 1.5 which helps us in achieving a good resolution.
- Under one case i.e. human heart beat detection frequency points chosen were 889. As step duration of single frequency point is 45 us and 889 frequencies points that give required sweep time period 40 ms. This will be discussed in detail in section 3.5.2.
- The power level is chosen to be 20 dBm so that penetration capability of the signal through the wall increases. Targets kept at large distances from the radar can also be detected.
- A double ridged waveguide horn antenna has been chosen which operates in the chosen frequency range and provides a good gain of around 10 dBi.

Chapter 2

Literature Review

A state of the art TWI system was presented by Ferris and Currie and they expected that advancement of field will take place in next ten to fifteen year at that time (1998) [1]. They discussed different imaging and non imaging sensors with their capabilities for through wall surveillance. This land mark paper tells about various available techniques for military surveillance. They explained tradeoff between bandwidth and power for Radar systems, attenuation of signal with higher frequencies. Selection of frequency range is one of the important parameter in radar. Selecting higher frequencies allow large bandwidth but at the same time penetration capability reduces. So selection should be done carefully. The researchers have used different frequency ranges for radar. Allan Hunt [16] has chosen 500 MHz to 2 GHz, Soldovieri et al., [28] worked in frequency range of 0.8 GHz to 4 GHz, Ahmad et al., [11] have worked in the range of 1 to 12.4 GHz and Dehmollaian and Sarabandi [6] have worked in the range of 1 to 3 GHz. The operational frequency band is 1 GHz to 3 GHz following FCC regulation [13]. The advantage of using UWB is that it has a high relative bandwidth, that is high absolute bandwidth is provided at a smaller central frequency. Hence, the power-resolution tradeoff can be addressed to some extent. Preliminary experimental investigations on the application of UWB electromagnetic signals for through-wall detection are presented by Aittya *et al.* [30]. G Barrie [31] introduced Ultra Wideband Short Pulse (UWB-SP) synthetic aperture (SP) through wall imaging system. Image formation and data collection have been discussed. A prototype data collection system has been developed and presented. A signal model using fourth order Gaussian derivatives has been presented. Factors affecting the system performance have been discussed. For image formation, backprojection method has been presented. FBP (Filtered Back projection) and its advantages have been discussed [38].

In TWI, received signal consists of desired response of target along with additions of other signals arising mainly from radar system parameters, wall reflections, environment of room and multiple reflections. These unwanted signals are known as clutter. Clutters which are undesired component in the received signal mean those signals that are unrelated to the target scattering

characteristics but occur in the same sample time window and have similar spectral characteristics to the target signatures [34]. Radar system must be calibrated to remove systematic errors such as uneven frequency responses due to cables and antennas. Calibration is an important aspect for any radar system [5]. To improve the quality of detection and reduce false alarm, signal to clutter ratio must be increased. For optimal target recognition, clutter removed signal will be very helpful. Verma et.al [20] discussed various clutter reduction techniques to enhance the detection accuracy and reduce false target detection. A brief comparison based on the peak signal to noise ratio is carried out. They concluded that ICA is best clutter removal algorithm for detection of low dielectric target. When low dielectric target, such as Teflon is used then only ICA is able to detect target. One of the commonly used methods for clutter reduction in TWI relies on background subtraction, where two images taken with and without target are subtracted [32]. But this technique has a drawback because clutter remains present if the data is not collected at exactly the same antenna positions in both cases. In addition, it is not possible in real scenarios to collect data without target. Recently a spatial filter based clutter reduction technique is developed in which zero spatial frequency which represents wall reflections is notched from the image [33]. Spatial filters have been applied across the antenna array to significantly mitigate the spatial zero frequency and low frequency components which correspond to wall reflections. In further sections we will see a similar type of filter named moving target indicator used for heart beat detection. This filter may subtract low frequency components of target as well. This method removes reflections from wall but does not discuss about how reflections due to other non target objects (clutters) are reduced.

TWI radar detects any object that lie in its line of sight if the conductivity of object or dielectric constant or permeability is different from the surrounding medium. Since change in absorption mainly affects absorption so it is usually the contrast in the permittivity that leads to a reflection of the electromagnetic waves radiated by the transmit antenna. Metal target will reflect more energy and appears bright while target having low dielectric constant will reflect less energy and appear as if no target is there. Problem of detection of target due to low contrast is solved by morphological contrast enhancement technique and histogram equalization method. Not much work has been done in through wall imaging for target identification which includes both physical and geographical information i.e. the shape. Debes *et al.* [35] have solved the problem of automatic target classification for through wall imaging. First segmentation has been carried

out using the Iterated Conditional Modes (ICM) algorithm. After that, feature extraction has been performed using superquadrics. Super ellipsoids have been considered for this purpose.

CH Gierull [46] in a technical report submitted to DRDC stated that in military environments, monostatic synthetic aperture radar (SAR) is, due to it active illumination of the scene, easily detected and thus highly vulnerable to electronic counters measures or even destruction. He stressed on design of a bistatic/multi-static system. Xin et al [47] based on mathematical model developed by them remarked that bistatic radar provides greater diversity in aspect angle than monostatic radar and acquiring more scattering information, which is competent for imaging of a building. They analyzed Doppler, 2-D resolution and wall effects based on their bistatic radar simulation and concluded that velocity of the transmitter greatly affects the Doppler FM rate. Bistatic range history is azimuth dependent, value of Doppler rate and azimuth resolutions are range dependent, Wall effects on the overall 2-D resolution distribution are negligible. Akduman et.al [36] worked on target detection of targets using antenna in bistatic mode with two step strategy. First one is localization of the target and second is imaging.

Narayanan et al [42] developed an UWB random noise RADAR for moving target detection. For a through-wall applications this noise radar using array antennas, subtraction of successive frames of the cross-correlation signals between each received element signal and the transmitted signal is able to isolate moving targets in heavy clutter. Human activities are usually detected by the Doppler shifts associated with the human's heartbeat, breathing, walking, arm waving, etc., using Doppler radar. For tracking moving targets they combined Doppler processing with filtered backprojection. It is capable of precisely tracking the moving target but being computationally complex and due to huge hardware requirement (40 receivers) it was not used by us. Nag et al.[43] worked on time modulated UWB impulse radar model. Time modulation indicates pulse position modulation which varies the inter-pulse period of the transmitted short time duration pulses. It was used to generate two-dimensional (2D) Interferometric Images of moving targets. It was designed to overcome the limitation with Time Domain Corporation (TDC) radar system which provides response to a moving target only along the down-range direction. That radar does not provide any azimuth bearing information other than that which can be gleaned from its rather wide 90 degrees beam-width. However Radar made by Nag et. Al is capable of detecting in azimuthal direction too and can both standing and crawling human.

Starderini [18] studied the use of UWB radars for medical applications and differentiated between ultrasound electromagnetic pulses and UWB radar. In details he described Micropower Impulsive Radars (MIR) and its advantages over traditional ultrasound sensors and electrocardiogram such as no physical contact is needed. Gabriel [19] worked on the compilation of dielectric properties of biological tissue especially of humans which is very helpful while studying effect of radiation. He explained the dielectric model of human which is of great efficacy in case of understanding multiple reflections occurring while radiation is incident on thorax region.

A hybrid technique is presented by Scott [40] that simultaneously uses both electromagnetic and acoustic waves in a synergistic manner to detect buried land mines. The system consists of electromagnetic radar and an acoustic source. The acoustic source causes both the mine and the surface of the earth to be displaced the electromagnetic radar is used to detect these displacements and, thus, the mine. Ivashov et al [41] named the method as vibro-electromagnetic sounding. Their research was limited to detection and diagnostics of a live person by detecting its mechanical vibrations. This method produced excellent results in detection of heart beat, breathing and talking frequency but does not provide any information about range of the target.

S. Jefremov and B. Levitas [39] demonstrated the use of impulse radar to detect heart-beat by employing a 30 ps pulse. SFCW radars provide us with range and Doppler information unlike CW pulse radars, which cannot give range information. A low cost device using CW Doppler radar was described by M. Jelen and E. M. Biebl [26]. Reference [27] illustrates the use of blind source separation to separate two heart-beats detected by single-tone Doppler radar. Zhou Yong et al [22] worked out new theoretical method to obtain the range and Doppler frequency of human body is proposed in which multiple periods stepped frequency continuous-wave signal and moving target indication (MTI) filter are adopted. They used stepped-frequency continuous-wave and adopted multiple periods signal and MTI filter to extract Doppler frequencies and range of human body which are in the echo modulated by the fluctuation of skin caused by heart beating and breathing. The overall process used by them is known as Range-Doppler Processing. Mahafza [24] worked on MATLAB implementation of single delay canceller and Recursive MTI which serves a great deal in implementation of MTI for heart beat detection.

Chapter 3

Experimental Setup & Methodology

3.1. Experimental Setup for Collection of Data

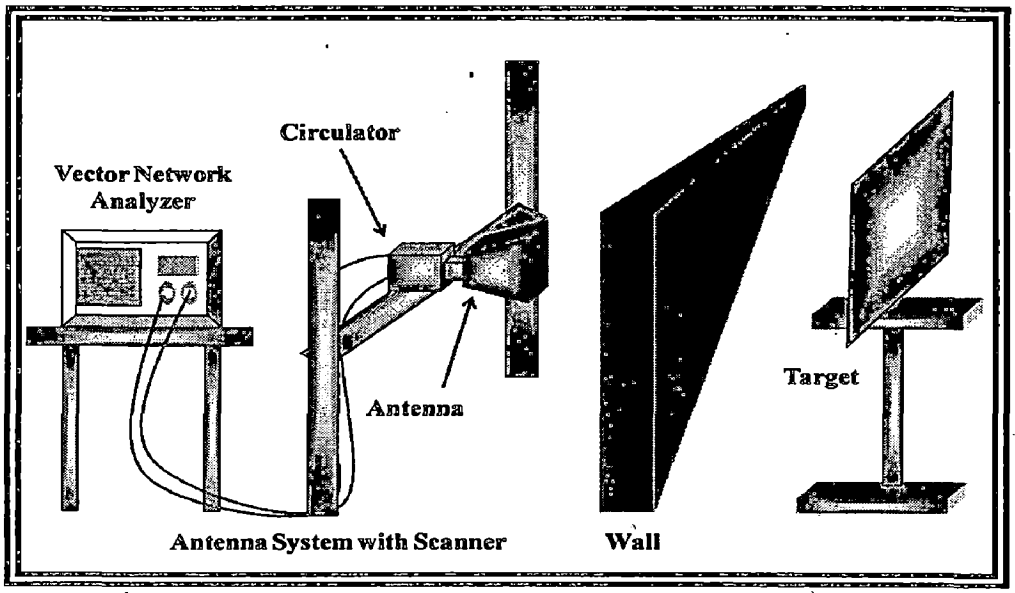

Figure 3.1: Experimental Setup[34]

Figure 3.1 shows the setup used for experimental work. VNA is used for calculation of S-parameters as well as RF source. Its data was transferred in real time to PC by interfacing. Waveguide horn antenna R&S HF 906 and HF 907 is used as the radar.

3.1.1. Constituents of the experimental setup:

(a) Vector Network Analyzer (VNA)

Variety of parameters including the amplitude response as well as the network scattering parameters, or S-parameters, which are the transmission and reflection coefficients for the device under test are measured by VNA. These S-parameters contain both amplitude and phase

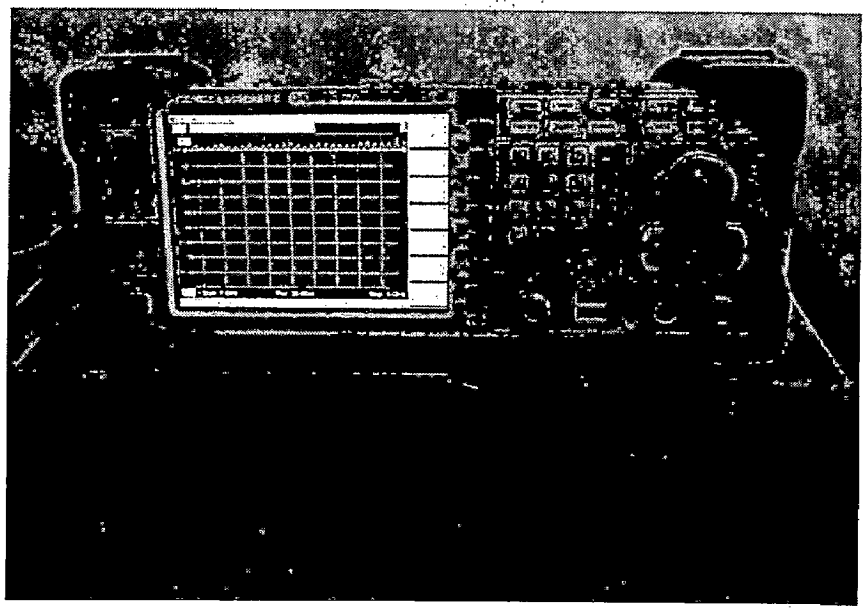

Figure 3.2: Vector Network Analyzer

information, and therefore a vector network analyzer, VNA (shown in Figure 3.2) is able to give a very comprehensive view of the device. The vector network analyzer used in this experimental work is Rhode and Schwarz VNA (R&S ZVL 132). It generates frequencies in the range of 9 kHz to 3 GHz. It is capable of giving power level of 20 dBm. In this work VNA was used for reflection measurement. In a reflection measurement, the analyzer transmits a stimulus signal to the input port of the device under test (DUT) and measures the reflected wave. In this work, the VNA was operated at frequency range of 1GHz- 3GHz and number of frequency points was 201. The VNA was used as a source of RF power as well as to measure the S Parameters.

(b) Antenna

The horn antenna may be considered as an RF transformer or impedance match between the waveguide feeder and free space which has an impedance of 377 ohms. By having a tapered or having a flared end to the waveguide the horn antenna is formed and this enables the impedance to be matched. Although the waveguide will radiate without a horn antenna, this provides a far more efficient match. However the main advantage of the horn antenna is that it provides a significant level of directivity and gain. For greater levels of gain the horn antenna should have a large aperture. Also to achieve the maximum gain for a given aperture size, the taper should be long so that the phase of the wave-front is as nearly constant as possible across the aperture [38].

Thus the radiation characteristics depend on the flare angle, aperture dimension, type of flare, length of the flare etc. The lowest frequency of operation of a horn is fixed by the cut-off frequency of the waveguide and the neck dimension.

For antenna in bistatic mode operation (oriented target detection) we use 2 Rohde and Schwarz HF 907 double ridged waveguide horn antenna (in bistatic mode as shown in Figure 3.9) with linear polarization, which is a broadband compact transmitting and receiving antenna for the frequency range 1GHz to 18 GHz. However Antenna is used in monostatic mode for other majority of other data collection.

Table 3.1 Antenna specifications (From R&S Antenna Manual)

Specifications	**R & S HF 907**	**R&S HF 906**
Frequency range	1 GHz to 18 GHz	800 MHz to 18 GHz
polarization	Linear	Linear
RF connector	N female	N female
Nominal impedance	50 Ω	50 Ω
Gain	5 dBi to 14 dBi	7 dBi to 14 dBi
VSWR	< 2.5	< 2.5
Max. RF input power	300 W between 0.8-4.5 GHz 200 W at 10 GHz 150 W at 18 GHz	300 W CW , 500 W PEAK
Max . height	226 mm	160 mm
Max . width	305 mm	250 mm
Max . length	280 mm	290 mm
Weight	1.9 kg	1.5 Kg
MTBF	>100.000 h	
Rated temperature range	-10°C to + 50°C	-10°C to + 50°C
Storage temperature range	-40°C to +70°C	-40°C to +70°C

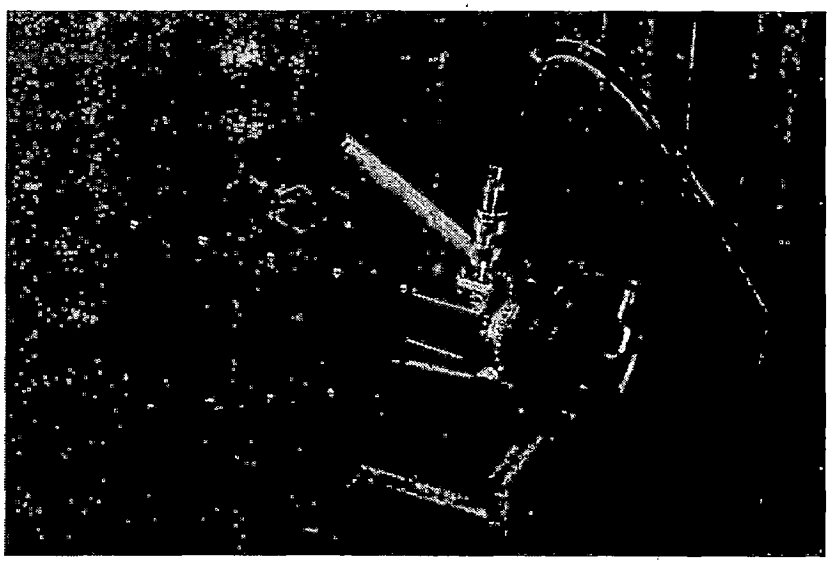

Figure 3.3: Waveguide Horn Antenna HF 906

Figure 3.3 shows the waveguide horn antenna R&S HF 906 used for experimental work. This is the common antenna used for antenna in monostatic mode readings. HF 907 is used for data collection in bistatic mode.

(i) Beamwidth of the antenna:

Half Power Beam Width (HPBW) of the antenna is needed to calculate the swath of the antenna used. The beamwidth of the antenna used in the H Plane and E Plane is 80 degrees and 100 degrees respectively at centre frequency.

(ii) Swath:

The Swath becomes a very important parameter for Through Wall Imaging applications as it determines the area which is illuminated by the antenna in a particular plane at a certain distance from the antenna. The Swath is an elliptical area whose value depends on the HPBW of the antenna and the distance at which imaging is to be performed.

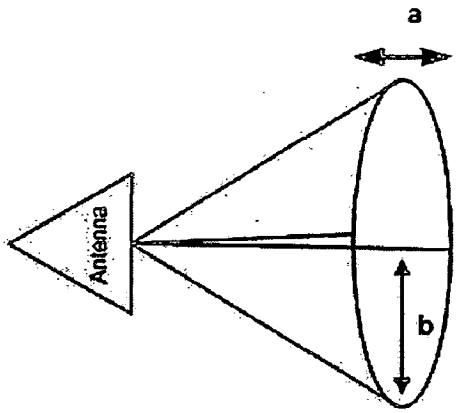

Figure3.4: Swath of TWI Radar

The swath as shown in Figure 3.4, Δ at the investigated depth d from the antenna is given by:

$$\Delta = \pi ab \tag{3.1}$$

Where a is semi-minor axis,b is the semi-major axis of the ellipse d is the distance at which swath is to be calculated. The values of a and b is calculated by equations given below:

$$a = d \tan\frac{\theta_a}{2} \tag{3.2}$$

$$b = d \tan\frac{\theta_b}{2} \tag{3.3}$$

Therefore,

$$\Delta = \pi d^2 \tan\frac{\theta_a}{2} \tan\frac{\theta_b}{2} \tag{3.4}$$

As $\theta_a = 80^\circ$ and $\theta_b = 100^\circ$, at investigated depths as measured from antenna flare swath area are 1.77 m^2 for d=0.75 m, 3.14 m^2 for d = 1 m.

(c) Scanner

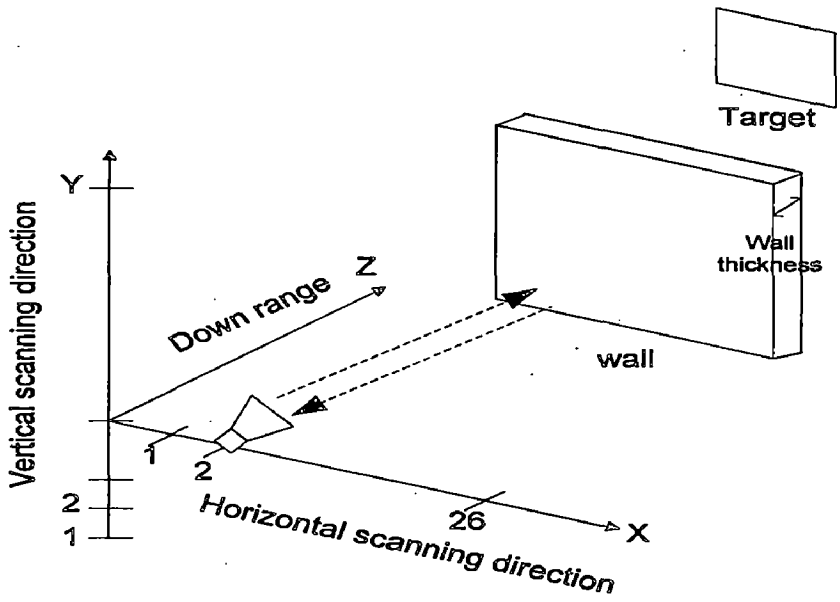

Figure.3.5: Scanner for collecting Data [34]

For scanning purposes a wooden scanner as shown in Fig. 3.5 is used to position the radar at different locations so that the scene to be imaged could be illuminated completely. The scanner used has 30 positions in the horizontal direction and 20 positions in the vertical direction. The spacing between successive positions in the horizontal as well as vertical direction was 0.05 m.

(d) Personal Computer

A SONY laptop is used which is connected to the Vector Network Analyzer (VNA) using a LAN connection. The PC is important for real time implementation. The software used is Math works MATLAB. Virtual Instrument Software Architecture (VISA) provided by National Instruments (NI) was used to provide an interface between hardware (VNA) and the development environment (MATLAB). It was critical for implementation of TWI techniques in real time.

3.1.2. Data Collection:

Closely observing the advantages of Stepped Frequency Continuous Wave (SFCW) radar, this system is used to collect the data used in this work. The data is collected at 201 frequency points in the frequency range of 1 GHz- 3GHz. The methodology of data collection is discussed below.

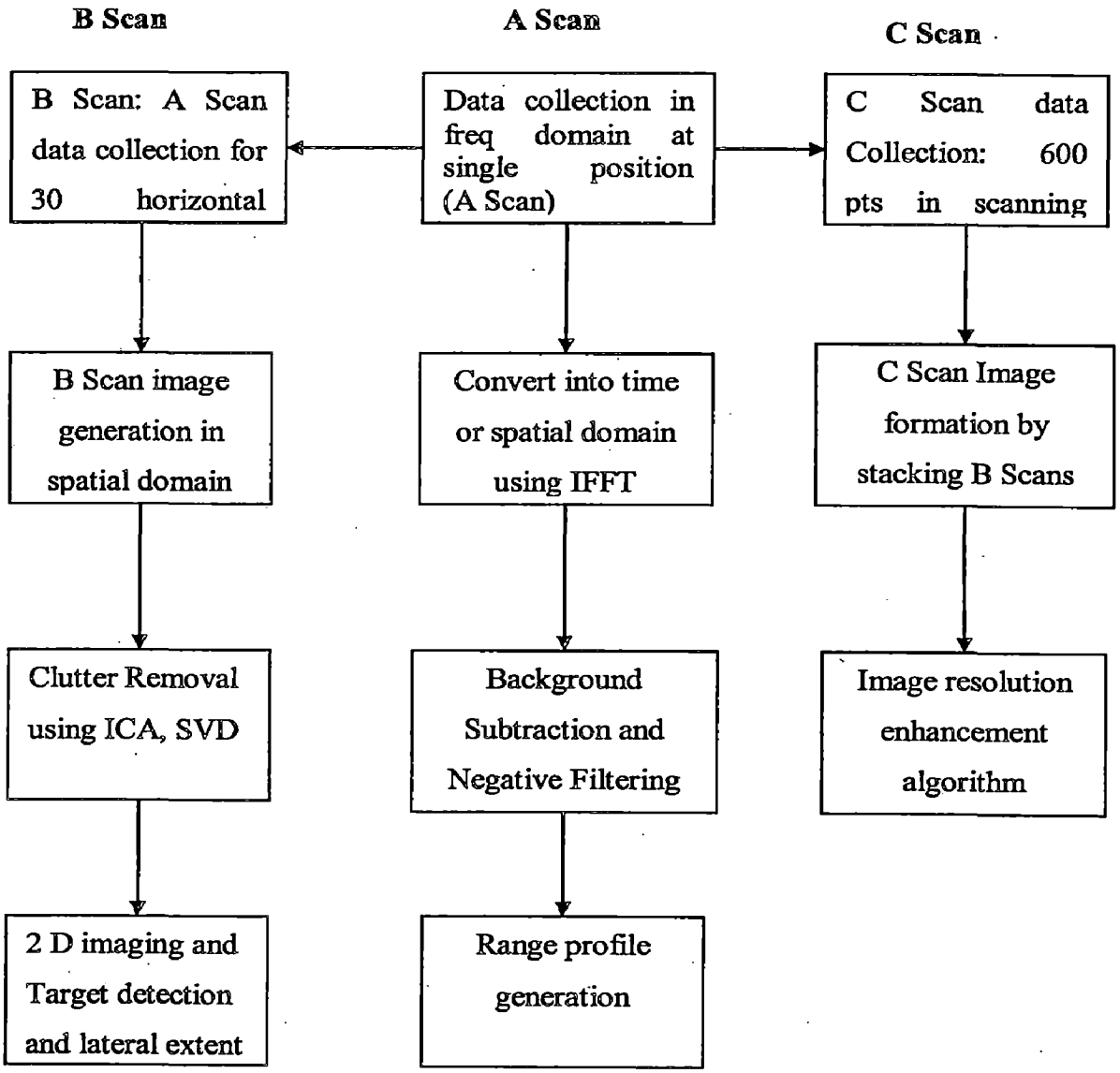

Figure 3.0.6: Flow chart of A, B and C Scan

Pre-processing of the collected data mainly consists of 1) frequency to spatial domain 2) calibration and 3) velocity correction. Before detection process, pre-processing techniques are applied.

Post processing consists of operation that we apply on generated image like clutter removal techniques Singular Value Decomposition (SVD), Independent Component Analysis (ICA). Clutter is present due to reflections from objects other than the target and other sources like reflection from the wall. Low dielectric target like human is successfully detected after application of clutter reduction technique Independent Component Analysis (ICA).

Figure 3.6 shows a comprehensive flowchart of the approach used for model development. A brief description is as follows:

- The process of collection of data is carried by scanning the radar and placing it at different locations. Different types of data collection are: A Scan, B Scan and C Scan. They are explained in detail later. Also different clutter reduction techniques such as Singular Value Decomposition (SVD), Independent Component Analysis (ICA) [20] etc. can be applied.
- There are two common modes of antenna operations, one is monostatic mode and other is bistatic mode. In monostatic mode there is single antenna acting as transmitter and receiver whereas in bistatic mode there are separate transmitter and receiver. The C Scan image generation for these kinds of targets by stacking B Scan images. Its resolution I enhanced by using MATLAB commands.
- Talking about detection of activities behind the wall moving target detection is our prime interest. An iterative time domain A Scan gives us the clear picture of the target movement. Details will be discussed in later section 3.4.

Apart from these, repetitive 250 A Scans with increased number of frequency points is required for detection of metabolic activities of human like heart beat as aggregate sweep duration of about 40 ms is required for 250 total sweeps. This is discussed in section 3.5.2.

Table 3.2 shows the various system parameters whose numerical value will be used in the subsequent section of the report.

Table 3.2: System parameters used for data collection.

VNA	R&S ZVL	1 GHz – 3GHz
Frequency Points		201
Antenna	Double-ridged waveguide type (HF 906)	800MHz-18 GHz
VNA Power		20 dBm
Range resolution	$\Delta R = c/2N\Delta f$	7.5 cm
Azimuth resolution	$\Delta CR = \lambda D/R$	14.9 cm
Cable Loss(1GHz-3GHz)		1.0 dB-1.5 dB
Unambiguous range	$R=c/2\Delta f$	300 m
Antenna-air reflection		0.225 m
Wall thickness, dielectric	Calculated in the lab	0.125 m, 5.3

The antenna is connected to the VNA using coaxial cable and the antenna is positioned on the scanner for data collection. There are three different kinds of 'scans' that can be performed:

A Scan: Basic level which provides information about presence of target along with approximate location of the target is called as A-scan or range profile. But it does not indicate how many targets are present in cross range. Details of this algorithm are discussed in section 3.2

B Scan: B Scan consists of one complete scan along the horizontal direction (30 positions). It provides information about the target lateral extent along the crossrange in addition to the target location in the downrange direction. In monostatic case, radar transmits and received the signal and then moves to the next location and repeat operation along a predefined path in front of wall.

It also provides information about number of targets presents in cross range along with their exact locations.

C Scan: C scan corresponds to placement of the radar on all the possible locations (30X20). It can be used to find out the two dimensional shape of the object and can be extended to 3 D image formation. It is generated by stacking B Scans in order of their heights.

Figure 3.7 explains the concept of 2D and 3D imaging. When we have target information in the horizontal grid lying in the crossrange-downrange plane, it corresponds to B-scan or 2D imaging. When we have target information along the vertical grid at a particular downrange distance, it is called as 3D imaging as we have information regarding the target in all three directions

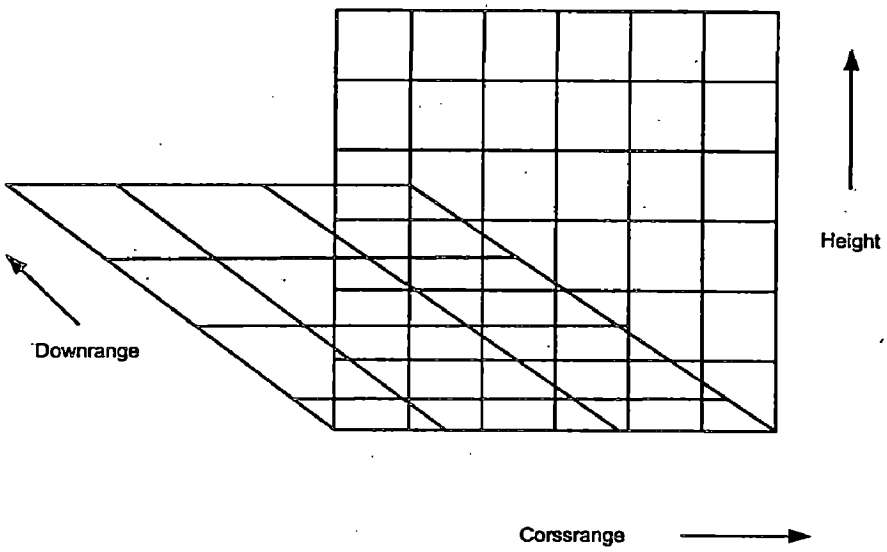

Figure 3.7: Grid for 2 D and 3 D imaging for TWI [38]

3.2. Processing of Data:

Step 1: VNA Calibration

Calibration process eliminates systematic, reproducible errors from the measurement results. Calibration plays an important role in determining the accuracy of the measurement system [5]. The process involves the following stages:

1. A set of calibration standards is selected and measured over the required sweep range.
2. The analyzer compares the measurement data of the standards with their known, ideal response. The difference is used to calculate the system errors using a particular error model (calibration type) and derive a set of system error correction data.
3. The system error correction data is used to correct the measurement results of a DUT that is measured instead of the standards.

Depending on the requirement of mode of operation one port and two port calibration can be done. For one port calibration open, short and match load matching is performed whereas for two port calibration open port calibration is performed for each port and then through port matching is done. This is commonly known as TOSM matching.

Table 3.3: Channel setting in VNA

Calibration	Full 2 port
Parameter	S_{21}, S_{11}
Start frequency	1 GHz
Stop frequency	3GHz
Number of points	201
Power	20 dBm

Step 2: A Scan Algorithm [38]:

The data collected by the VNA is in the frequency domain at frequency points f_n which is converted to the time domain by inverse fast Fourier transform (IFFT). Mathematically, a signal returned from a target at a distance in the frequency domain is given by equation:

$$s(f_n) = \frac{1}{\tau_{max}} \int_0^{\tau_{max}} S(t) \exp(-j2\pi f_n t) dt \tag{3.5}$$

$$\Delta\tau = \frac{1}{N_f \Delta f} \tag{3.6}$$

$$\tau_{\max} = \frac{N_f - 1}{BW} \tag{3.7}$$

Where $\Delta\tau$ is the time resolution possible with the stepped frequency waveform of N_f uniform steps of Δf, $\tau_{\max}$ is the maximum time possible and BW *is* the bandwidth of the system. For the present case, $N_f = 4001$ and $\Delta f = 0.5$ MHz Thus we see the need to choose $N = 4001$ for increased resolution. The signal obtained in frequency domain is converted into time domain by performing inverse Fourier Transform. The time domain signal is represented as:

$$s(t) = \sum_{n=0}^{N_f - 1} S(f_n) \exp(j2\pi f_n t) \tag{3.8}$$

Mapping from time domain to spatial domain is done according to following equation:

$$z = \frac{ct}{2} \tag{3.9}$$

The mapped spatial domain signal is represented as:

$$s(z) = \sum_{n=0}^{N_f - 1} S(f_n) \exp\left(j2\pi f_n \left(\frac{2z}{c} \right) \right) \tag{3.10}$$

Step 3: Calibration using metal sheet

The reflection that occurs at the antenna air reflection can be removed by performing calibration using a metal sheet. It helps in shifting the location of the target to the position which is closer to its true location. The metallic sheet is kept at the antenna flare and then the first dominant reflection that is observed corresponds to the delay encountered by the wave up to the antenna-air interface point [44]. Data can be time-gated up to the index value so observed. The corrected signal is given by:

$$s(t, t_{ref}) = \sum_{n=0}^{N-1} S(f_n) \exp(j2\pi f_n (t + t_{ref})) \tag{3.11}$$

$$s(z,R_{ref}) = \sum_{n=0}^{N-1} S(f_n) exp(j2\pi f_n (2z/c + 2R_{ref}/c)) \tag{3.12}$$

t_{ref} and R_{ref} correspond to the metal sheet kept at the antenna flare.

Step 4: Velocity Correction [45]

The signal slows down while it travels through the wall which results in a shift in the target location when target detection is done. This shift in the target location is compensated by employing 'velocity correction [45]. The knowledge of the wall's dialectic constant and thickness is required for the correction.

For non magnetic material walls the relative permeability is equal to one. Therefore:

$$v_{wall} = \frac{c}{\sqrt{\varepsilon_{rwall}}} \tag{3.13}$$

$$t_{delay} = \frac{D_{wall}}{v_{wall}} - \frac{D_{wall}}{c} = \frac{D_{wall}}{c}(\sqrt{\varepsilon_{rwall}} - 1) \tag{3.14}$$

Where D_{wall} is the distance travelled inside the wall and is the relative permittivity of the wall.

The final corrected signal is given by:

$$s(t,t_{ref},t_{delay}) = \sum_{n=0}^{N-1} S(f_n) exp(j2\pi f_n (t + t_{ref} + t_{delay})) \tag{3.15}$$

$$s(z_{final}) = s(z,R_{ref},z_{delay}) = \sum_{n=0}^{N-1} S(f_n) exp(j2\pi f_n (2z/c + 2R_{ref}/c + 2z_{delay}/c)) \tag{3.16}$$

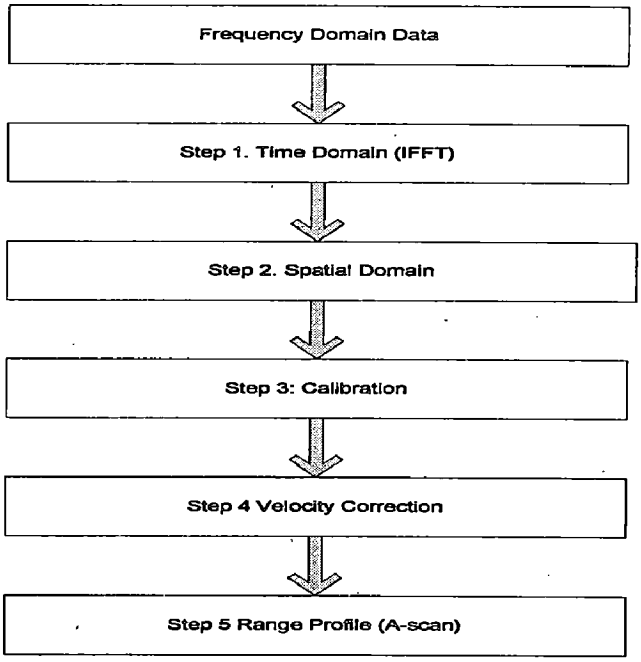

Figure 3.8: Flowchart for A Scan algorithm [34]

Step 5: B Scan image generation

Data collection at 30 consecutive horizontal positions along the scanner constitutes B Scan as shown in Figure 3.7. The data collected is converted to time domain in the similar way as A Scan for each individual radar location, and then the MATLAB function imagesc is used to generate a simple B Scan image. This is commonly known as raw B Scan image.

Step 6: C Scan image generation

Starting from ground level; B Scans are repeated with increasing height levels up to the height of the target under scan. For example, in our experimental setup 20 B Scan are performed with successive increase of 5 cm in vertical direction.

After these steps known as preprocessing, the data in post processed to remove unwanted response. **Post processing** consists of operation that we apply on generated image like clutter removal techniques Singular Value Decomposition (SVD), Independent Component Analysis (ICA). In raw data, various reflections other than that corresponding to the target can be

observed. The presence of objects other than the target, multipath propagation, wall reflection etc. is sources of clutter. The presence of clutter may make the detection of target difficult and impossible at times. Hence, various clutter reduction techniques were employed to improve target detection and visibility. Low dielectric target can be successfully detected after application of clutter reduction technique Independent Component Analysis (ICA).

3.3. Methodology for Oriented Target detection

The aim of this experiment was to do comparison between oriented target detection by antenna in monostatic mode and antenna in bistatic mode. In antenna in monostatic mode operation; single antenna acts as transmitter as well as receiver. However when antenna is used in bistatic mode; one antenna acts as transmitter while the other acts as receiver. The target (8'' radius metallic circular plate) was initially placed parallel to wall at a distance of 50 cm and then oriented by successive steps of 10 degree up to 40 degree and data was collected. The upcoming sub-sections describe the experimental set-up and data collection methodology for both kinds of modes.

3.3.1. Data Collection for Oriented Targets by using Antenna in Monostatic Mode.

(a) Experimental Setup

The antenna is connected to the VNA using coaxial cable and the antenna is positioned on the scanner for data collection. Antenna was operated in monostatic mode. Then calibration was performed by selecting simple 1-port calibration and using calibration kit ZVL 132 as described in step 1 of section 3.2. Further, interfacing of VNA with Laptop via LAN cable was done using VISA objects by National Instruments and MATLAB as platform

(b) Scanning

Firstly the target was set parallel to wall at distance of 50 cm and antenna to wall distance was 40 cm. One-dimensional information of target is known as A-scan that will only provide downrange information. However, in this experiment synthetic aperture radar imaging concept is used to get fine crossrange resolution. To emulate a large aperture by moving single antenna in monostatic mode called as B-scan. The scattering parameter which will be collected in this

experiment is S11. After confirmation of target by B-Scan; C- Scan is performed. C scan corresponds to placement of the radar on all the possible locations (30X20). It can be used to find out the two dimensional shape of the object and can be extended to 3 D image formation. The target is further oriented in steps of 10 degree up to 40 degree with repetition of C Scan.

3.3.2. Data Collection for Oriented Targets by using Antenna in Bistatic Mode.

(a) Experimental Setup

The antennas are connected to the VNA using coaxial cable and the antenna is positioned on the scanner for data collection. Antenna was operated in bistatic mode. For this purpose two antennas are kept at a distance $\lambda/2$ as shown in Figure 3.9 just to make sure there is no crosstalk. Then VNA was calibrated by selecting 2-port TOSM i.e. Through, Open, Short, Match calibration and using calibration kit ZVL 132 as described in step 1 of section 3.2. Further, interfacing of VNA with Laptop via LAN cable was done using VISA objects by National Instruments and MATLAB as platform.

(b) Scanning

Firstly the target was set parallel to wall at distance of 50 cm. Scanning in this case is different from scanning by antenna in monostatic mode operation. For Scanning purpose one can move two antennas together [36] with constant separation or fix transmitter and move receiver. In my experiment antennas were moved together as shown in Figure 3.9 with separation of 20 cm to avoid crosstalk as mentioned earlier. Space was limited because of presence of two antennas, so number of scan points was limited to 20. The scattering parameter which will be collected in this experiment is S21. A coherent summation of data collected over a path will form a high resolution image known as two dimensional or B-scan image which is useful to know exact location of target and targets lateral dimension. After confirmation of target by B-Scan; C- Scan is performed. C scan corresponds to placement of the radar on all the possible locations (20X20). It can be used to find out the two dimensional shape of the object and can be extended to 3 D image formation. The target is further oriented in steps of 10 degree up to 40 degree with repetition of C Scan.

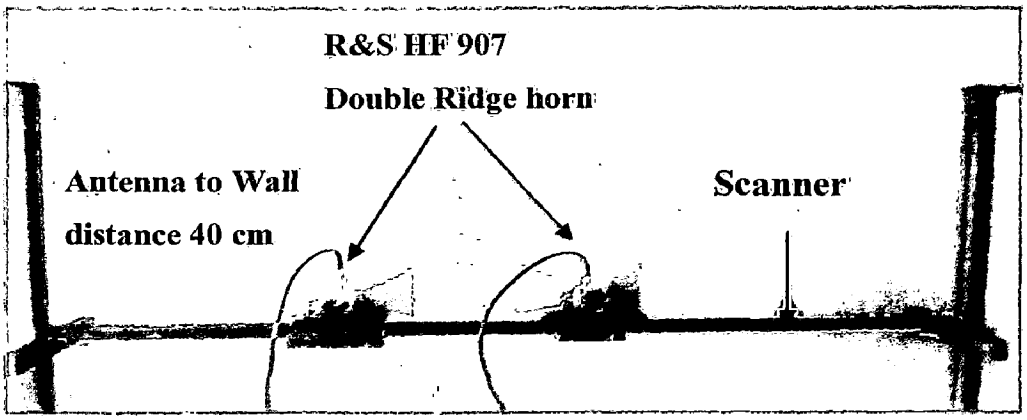

Figure 3.9: Antenna in Bistatic mode

3.3.3 Brief Note on Real time Processing

An interactive Graphic User Interface was prepared for the purpose of real time data collection. For B scan, a beep is produced by the system after which the antenna is moved onto the next horizontal location. In this way, after data collection is done along all the 30 or 20 positions depending on mode of operation and by application of inverse Fourier transform; the complex frequency domain data was converted into time domain and further into spatial domain. Hence the B Scan Image is generated. Then 20 such B Scans were performed at increasing levels constituting a C Scan. Then such C scan is repeated for circular target oriented (as shown in Figure 3.10) at 10, 20, 30, 40 degree to get respective 2-D shapes. The respective C Scan images formed by both methods are then compared. Flow chart of this entire process is shown in next subsection.

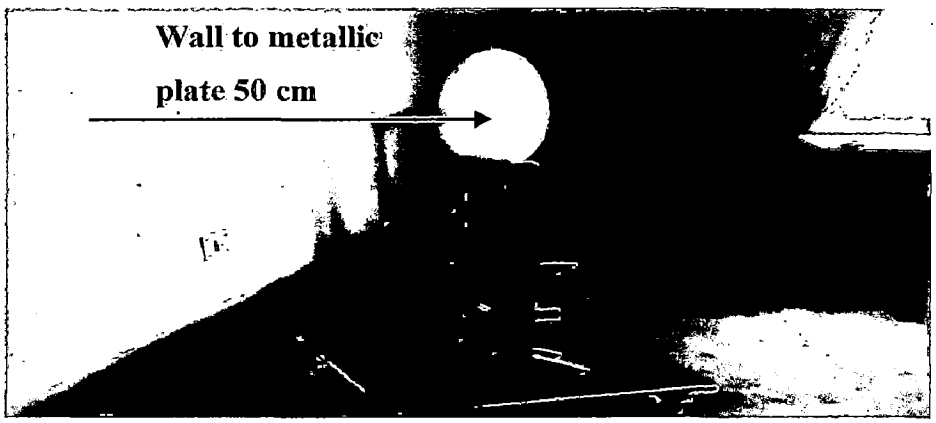

Figure 3.10: Metallic plate target oriented at 30 degree

3.3.4. Flow Chart for oriented target detection

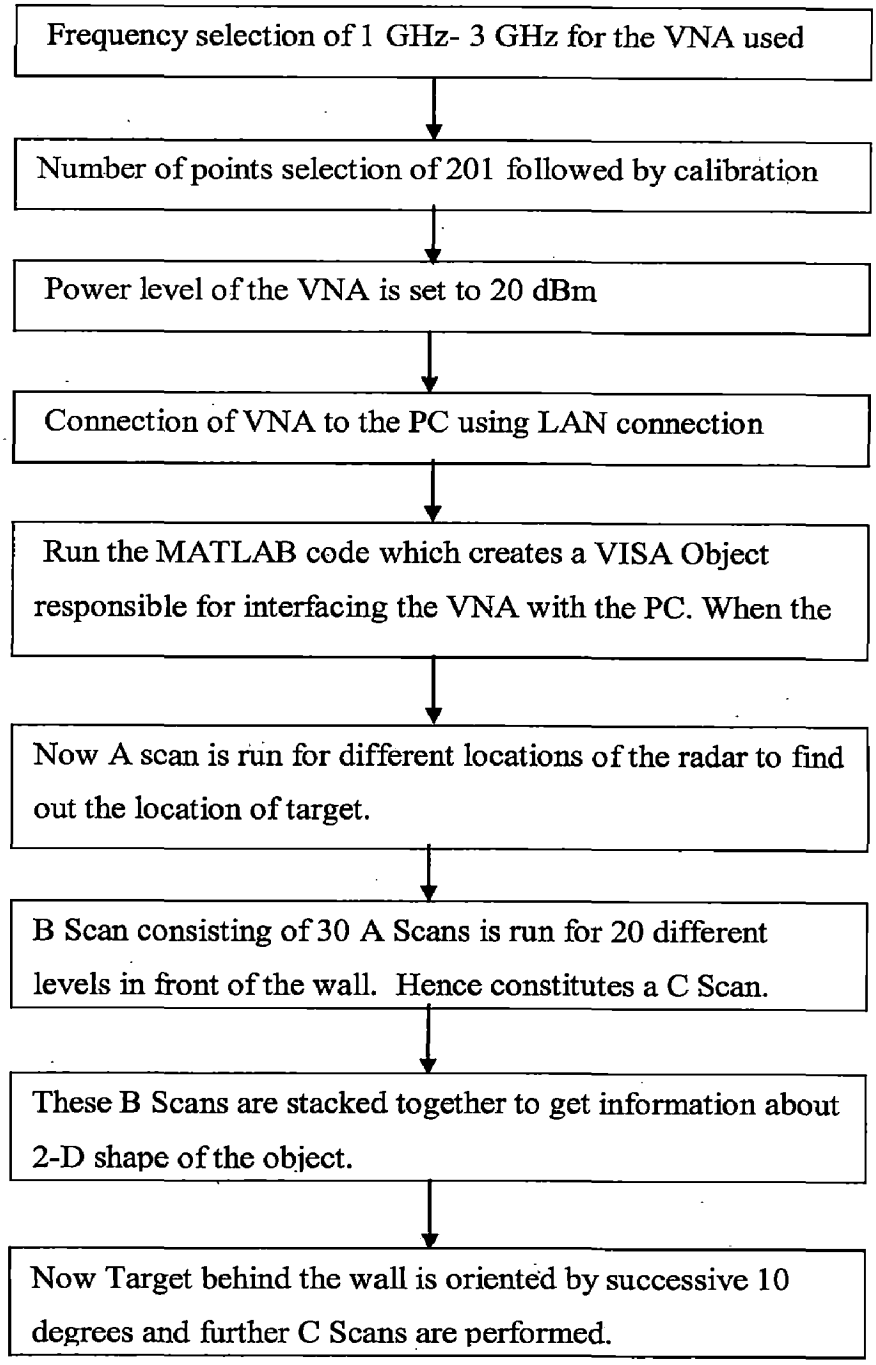

Figure 3.11: Flow chart of oriented target detection

3.4. Methodology for real time moving target detection

Earlier work in the field of Through Wall Imaging was concentrated on detecting stationary targets. Moving target behind the wall normal to its surface can be detected using iterative algorithm. Moving targets are mainly classified into two categories viz. living and non-living. Non-living moving targets especially metallic targets like robots, metallic plates are detected due to good reflection. Humans on the other hand are tough to detect. Methodology to detect both is discussed in brief.

3.4.1 Movement of the target

Experimental setup for the scanning side of wall for detecting moving metallic target is same as discussed in section 3.3.1 (a) for the case of oriented target detection. For stationary target detection; target is fixed and antenna moves on scanner. Contrary to that procedure; in this experiment antenna is fixed at one scanning position while the target moves on the other side of the wall. The movement is mainly in two directions.

(a) Downrange Movement

Downrange is the direction normal to the surface of the wall. So, downrange movement indicates motion of target in that direction. Initially, this movement was done in front of antenna's physical aperture from starting distance 30 cm till 2m from wall. This movement was then repeated at distance 20 cm, 40 cm, 60 cm away from antenna's physical aperture. The velocity of the metallic target was set as 20 cm/s while human takes 6 steps to cover distance of 2m in 3 sec and hence its speed was 2steps/sec

(b) Crossrange Movement

In this case target is set at a constant distance from the wall and moves parallel to the wall maintaining a constant distance from it. This crossrange movement was performed at distances 30cm, 60cm, 1m, 1.5m, and 2m from the wall. The velocity of the metallic target was set as 15 cm/s while human takes 2steps/sec

(c) Sitting and Standing Motion of Human

Crossrange and downrange motion detection are the examples of target motion detection in horizontal or H-Plane of the antenna. Sitting and standing human on the other hand can be detected by motion sensing by antenna in its vertical plane or E-Plane. Magnitude of reflection due to standing human is greater than sitting human. This is because the RCS of a walking person is larger than that corresponding to the crawling person. A radar based on Time Modulated UWB technology is designed by Nag et al [42] is capable of distinguishing between standing and crawling human. In our experiment we intended to do so by using SFCW based TWI system.

3.4.2. Processing

UWB Random noise radar was simulated by Wang et al [42] for through-wall applications due to important advantages like covertness, immunity from detection, jamming, and interference. By subtraction of successive frames of the cross-correlation signals between each received element signal and the transmitted signal; is able to isolate moving targets in heavy clutter. For tracking moving targets they combined Doppler processing (used to detect human motion) with filtered backprojection. It is capable of precisely tracking the moving target but is computationally complex. Huge hardware requirement (about 40 receivers) puts a tough challenge ahead its design, fabrication and real time implementation. Preliminary Interferometric images of moving targets obtained using a Time Modulated Ultra-Wide Band Through-Wall Penetration Radar fabricated by Nag et al [43]. Despite all its excellent advantages this prototype at present does not generate images in real-time and hence the image are generated by MATLAB from collected data.

We are using radar based on SFCW principle in which temporal domain data (which was converted from frequency domain data collected by VNA) was plotted iteratively in a 2-D grid. Due to updated response this plot gives clear idea about motion of the target and looks like a video. This response was converted into spatial domain by multiplication by velocity of light and division by appropriate factor (2 for antenna in monostatic mode). Phase or velocity correction may be applied to tackle effect of delay due to antenna air reflection and wall respectively. The spatial domain response of human is very faint even when he is closer to wall. So, background

response need to be subtracted so as to make human movement detectable. On subtraction of background response; value of net signal amplitude becomes negative at some distances, which makes no sense. These values are set to zero with the application of negative filtering. Response of moving target or human was recorded in a video; upon watching which direction of movement and velocity was estimated and confirmed.

3.4.3. Flow chart of the algorithm

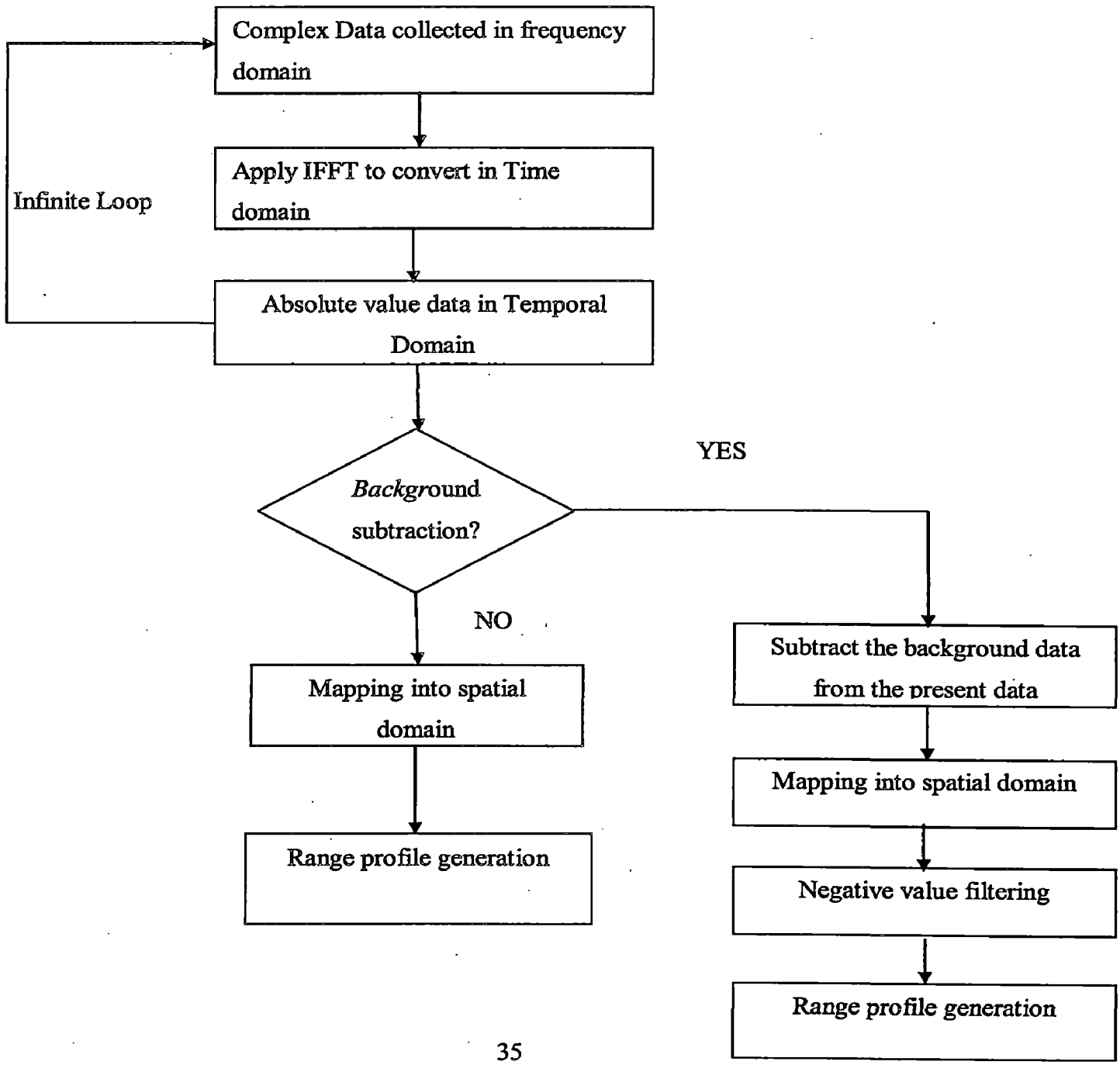

Figure 3.12: Flow Chart for Moving Target detection

3.5 Methodology for Human Heart Beat Detection

The overall conceptual working mode of a UWB radar system resembles that of ultrasonic echo transducers used in many applications. Electromagnetic pulses coming from UWB radar are able to probe the human body. The main and fundamental difference being that, contrary to ultrasound-electromagnetic pulses propagate through walls, ground, ice, mud, concrete, and the human body, as well. This is because there exist a definite difference in reflection magnitude between the heart muscle and the blood it pushes into the vascular tree. As the impedance of the cardiac muscle is on the order of 60 ohms and the impedance of blood is about 50 ohms, a roughly 10% reflection magnitude of the radio frequency energy at the heart muscle blood boundary can be expected. Similar reflection is taking place at air chest interface or chest/lung interface and even at vessel boundaries [18, 21]. The diagram shown below gives the clear picture of reflections taking place at various biological boundaries as EM radiation aimed at thorax enters the human body and penetrates all the way up to the heart. Losses at different boundaries are also shown in this Figure 3.13.

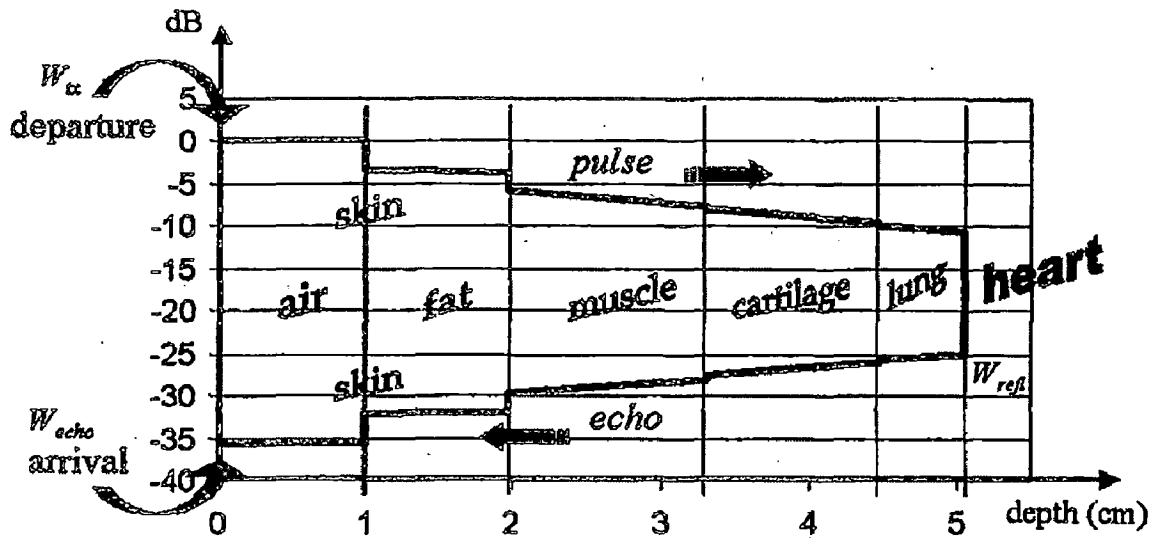

Figure 3.13: Attenuation at various biological boundaries for heart beat detection [18]

Table 3.4: Impedance, attenuation, speed and thickness of different physical layers while penetrating human heart [18]

	Impedance Ω	Attenuation m^{-1}	Speed m/s($x10^8$)	Thickness m
Air	377	0.00	2.998	1.00×10^{-2}
Fat	112.6	8.96	0.8958	0.96×10^{-2}
Muscle	49.99	31.67	0.3978	1.35×10^{-2}
Cartilage	58.16	31.93	0.4628	1.16×10^{-2}
Lung	52.86	29.62	0.4206	5.78×10^{-2}
Heart	49.17	38.71	0.3912	-

3.5.1 SFCW based Heart beat Detection

Stepped frequency continuous wave (SFCW) radars have gained momentum since the availability of fast frequency sweeping devices. Pulse radars have limitation that they can't give information about range and frequency simultaneously. Similar is the problem with vibro-electromagnetic radar. The principle is to utilize the phase modulation on the echo, and one widely used way of remote life detection is to use continuous-wave radar. The shift in position due to a minute Doppler (such as heart beat) changes the phase of the transmitted SFCW signal. Hence, the received voltage at the receiver is a function of phase. The process based on this phenomenon; Range Doppler processing is used. The stepped-frequency continuous-wave is used and multiple periods signal and MTI filter are adopted to extract Doppler frequencies and range of human body which are in the echo modulated by the fluctuation of skin caused by heart beating and breathing [22]. The Doppler phenomenon describes the shift in the center frequency of an incident waveform due to the target motion with respect to the source of radiation. Depending on the direction of the target's motion this frequency shift may be positive or negative. The fluctuation of skin caused by heart beating and

breathing can be thought as double-harmonic signal where the frequency of human breathing can range anywhere from 0.2 to 0.5 Hz and that of heart-beat can range from 0.8 to 2.5 Hz [23]. In average case heart beat of human can be assumed around 1.5 Hz and breathing rate can be considered as 0.5 Hz [6]. The bi harmonic range (distance from transmitter to human) function having complex reflection co-efficient discussed is given by this expression [22].

$$r(\tau) = r_0 + A_H \sin(\omega_H \tau + \phi_H) + A_B \sin(\omega_B \tau + \phi_B) \tag{3.17}$$

Where $\tau > 0$, r_0 is the average distance and A_H, A_B, ω_H and ω_B are amplitudes, angular frequencies and initial phases of heart beating and breathing respectively. The human being is assumed to be stationary. Hence, a signal with three frequencies can be expected from the human being; 0th frequency corresponding to the stationary part of the human body and two Doppler frequencies related to breathing and heart beat [6].

3.5.2 Method to detect heart beat with Moving Target Indicator

It is evident after looking at the response that the reflection due to walls is higher in magnitude compared to other objects. Static objects give a constant phase shift over a period of time compared to moving objects, due to which a high peak is formed at the 0th frequency after FFT. So to detect the human movement or heart beat movement and differentiate it from other stationary targets we need Moving Target Indicator or MTI. MTI is a kind of filter that suppresses the target-like response by clutter and allows response corresponding to moving target to pass through it with little degradation [24]. MTI filters can be implemented using delay line cancellers; simple one of these can be achieved by subtracting response of i th sweep from response of i+1 th sweep and is commonly known as single delay filter. In most radar applications the response of a single canceller is not acceptable since it does not have a wide notch in the stop-band. Delay line filters with feedback of recursive filters are solution to this problem. The advantage of a recursive filter is that through a feedback loop we will be able to shape the frequency response of the filter. A brief study and implementation procedure of single canceller and recursive filters is discussed in next page.

(a). Single Canceller

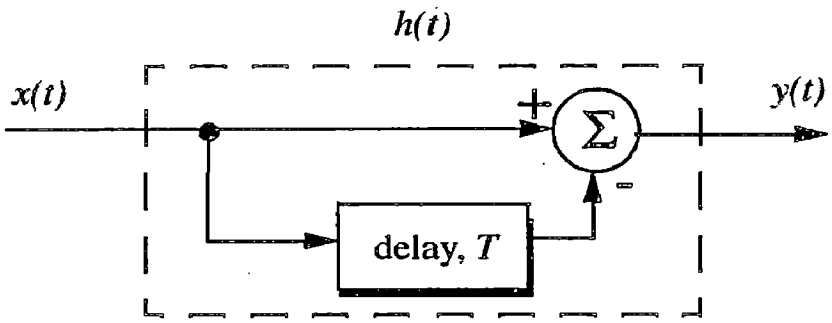

Figure 3.14: Single delay Canceller [24]

The canceller's impulse response is denoted as h (t). The output y (t) is equal to the convolution between the impulse response and the input x (t). The single delay canceller is often called a "two-pulse canceller" since it requires two distinct input pulses before an output can be read.

Here the output response will be given by

$$y(t) = x(t) - x(t-T) \tag{3.18}$$

Corresponding impulse response will be given as:

$$h(t) = \delta(t) - \delta(t-T) \tag{3.19}$$

Where δ is a delay function and Fourier transform of impulse response is given by

$$H(\omega) = 1 - e^{-j\omega t} \tag{3.20}$$

In the z-domain, the single delay line canceller response is

$$H(z) = 1 - z^{-1} \tag{3.21}$$

The gain of single canceller is given by

$$|H(\omega)|^2 = H(\omega)H^*(\omega) = (1-e^{-j\omega t})(1-e^{j\omega t}) \tag{3.22}$$

It follows that

$$|H(\omega)|^2 = 2(1-\cos\omega T) = 4(\sin(\omega T/2))^2 \tag{3.23}$$

From this it is clear that frequency response of single canceller is sine squared in nature. A plot of this response is shown in Figure 3.15. It is not acceptable since it does not have a wide notch in the stop-band. A good solution to this problem is recursive filter.

(b). Delay Lines with Feedback or Recursive filters

Delay line cancellers with feedback loops are known as recursive filters. The advantage of a recursive filter is that through a feedback loop we will be able to shape the frequency response of the filter. From Figure 3.15 we can write

$$y(t) = x(t) - (1-K)w(t) \tag{3.24}$$

$$v(t) = y(t) + w(t) \tag{3.25}$$

$$w(t) = v(t-T) \tag{3.26}$$

$$|H(z)|^2 = \frac{(1-z^{-1})(1-z)}{(1-Kz^{-1})(1-Kz)} \tag{3.27}$$

Using transformation $z = e^{j\omega t}$ and $z + z^{-1} = 2\cos\omega t$ we can write

$$|H(j\omega)|^2 = \frac{2(1-\cos\omega T)}{(1+K^2) - 2K\cos(\omega T)} \tag{3.28}$$

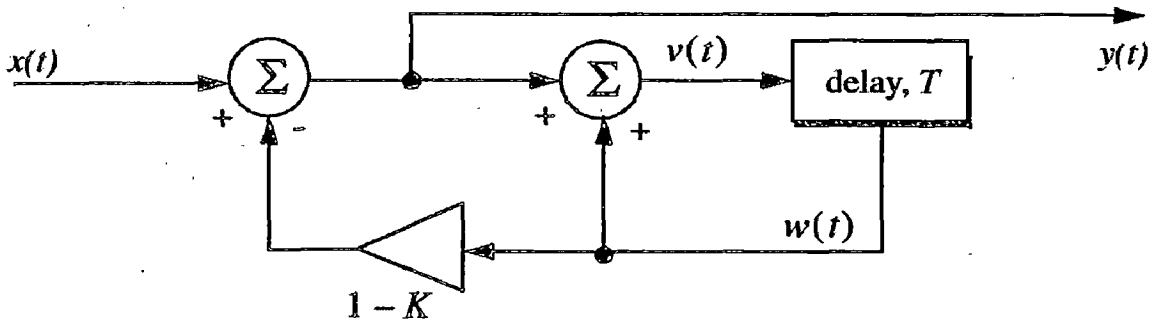

Figure 3.15: Recursive Filter [24]

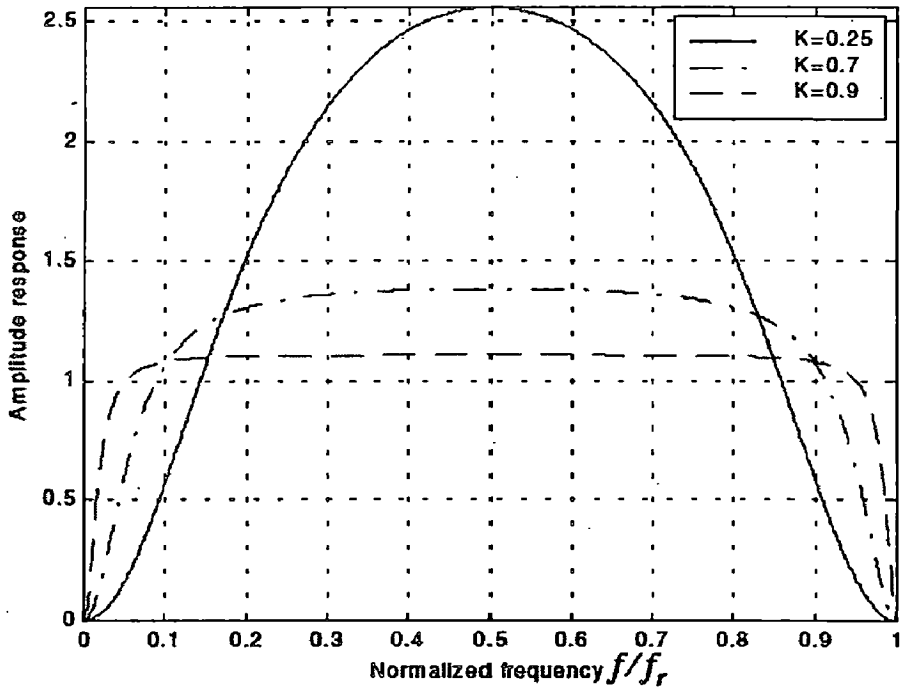

Figure 3.16: Frequency response of MTI for different values of K [24]

For k=0 this will reduce to a single canceller. Clearly by changing the value of K one can change the filter response. In order to avoid oscillation due to the positive feedback, the value of should be less than unity. The value is normally equal to the number of pulses received from the target. For example K=0.9 corresponds to ten pulses, while K= 0.98 corresponds to about fifty pulses. Figure 3.16 shows the plot of equation 3.23 for K = 0.25, 0.7, 0.9.

3.5.3 Experimental setup, Procedure & Parameters

(a) Experimental Setup

This experiment was conducted using Rohde & Schwarz ZVL vector Network Analyzer, R&S HF 906 double ridge horn antenna. Antenna was set at the height of human heart and about 40 cm from the wall. Thickness of wall (consists of bricks and plaster) is 12 cm. VNA was interfaced to PC and sweep data was acquired through MATLAB 7.6 using Virtual Instrument Software Architecture (VISA) objects.

Table 3.5: Parameter of RADAR for Heart beat detection

Parameter	Description
Frequency source	R&S Vector Network Analyzer
Antenna	R&S HF 906 (Double Ridge Horn Antenna)
Frequency Range	1-3 GHz
Range Resolution	0.075m
Transmitted Power	20 dBm
Number of Points	889
Step Duration	45 us
Sweep Period	40 ms
Sweeps	250
Total Scan Time	10 s

(c) Selection of Parameters

Selection of parameters for heart beat detection is very important part of the experimental procedure. Value of N or frequency points governs the sweep time of one frequency sweep of SFCW radar. Higher the value of N greater will be the sweep time. Further, greater will the value of N longer range will be covered. For achieving frequency step of 0.1 Hz in Range Doppler plane, sweep period should be around 40 milliseconds when M is selected 250. Frequency step duration of our VNA is around 45 microseconds. For this, number of frequency points should be 889 as explained.

Step duration = 45 us, Sweep time = 45us *889 = 40 ms

Value of parameter M or number of sweeps decides the frequency step size while plotting the collected data in Range Doppler plane. Larger value of M also ensures proper time for system to record heart beat. M equals to 250 gives a total scan time of 10s as explained.

Sweep time = 40 ms, Total scan period = 40ms * 250 = 10 s

These 10 seconds are enough to record at least one heart beat and one breath of the human. Thus intelligent selection of M and N increases the chances of heart beat detection.

(b) Procedure

Human stood initially at 30 cm from the wall and then in increasing steps of 10 cm up to 2 m. At one standing position radiation was incident for 10 s. For each scan, complex frequency domain data was stored in frequency domain. Inverse Fourier transform of this data along the rows is taken. Then FFT was taken along columns of this data. Data was plotted was proper scaling of the X and Y axis. This process is called Range Doppler Processing. In this image, due to stationary targets, maxima occur at 0^{th} frequency and heart beat frequency diminishes. When recursive MTI (discussed in 3.5.2(b)) filter was applied between the application of IFFT on rows and FFT on columns, then the resulting image will be able to detect heat beat. Results are discussed in section 4.4.

3.5.4 Flow Chart of Heart Beat Detection

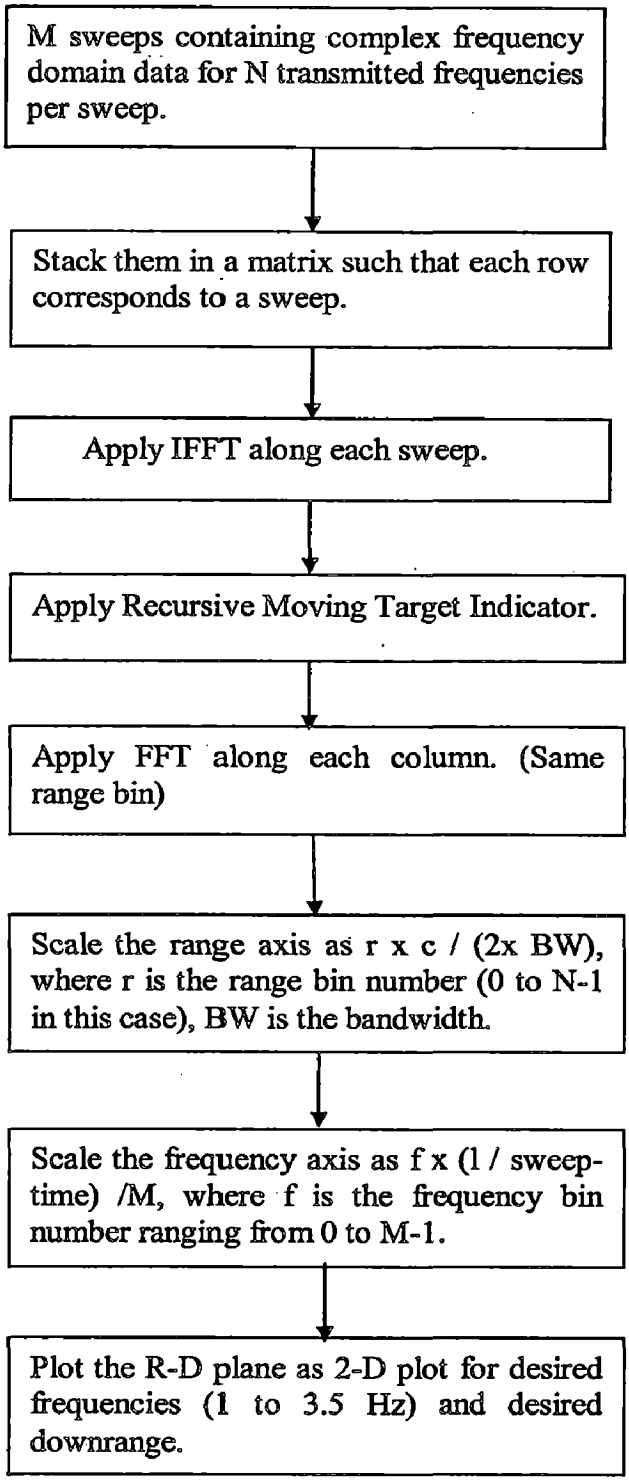

Figure 3.17: Flow chart of heart beat detection

Chapter 4

Implementation, Results and Discussions:

4.1. Oriented Target detection

With antenna in bistatic mode one can get fair idea about the shape of the target from C Scan image; but target is shifted away from its actual location in image. One can clearly see a continuous shift of the identified metallic plate in images shown in LHS. However the target remains at same location but oriented continuously. This happens due to orientation of target that transmitted radiations are received at far receiver. As angle of orientation increases there is greater shift of target in the image. Further if the angle of orientation is increased beyond 45 degree is becomes tougher to detect the target and antenna array will be required. On the other hand detection by antenna in monostatic mode is poor, since the shape is distorted, when compared to bistatic case. The **Height (Y axis) Vs Crossrange (X axis)** plot for different orientation for antenna in monostatic and bistatic mode is shown in Figures 4.2(a,b), 4.3(a,b), 4.4(a,b), 4.5(a,b).

Distance of Antenna from wall = 40 cm, Wall to target = 50 cm.

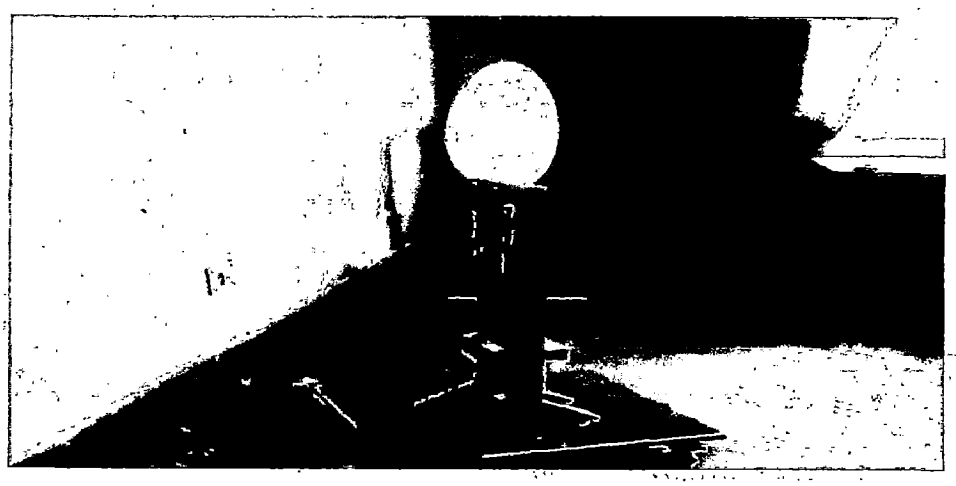

Figure 4.1: 30 degree oriented target

Antenna in Bistatic Mode **Antenna in Monostatic Mode**

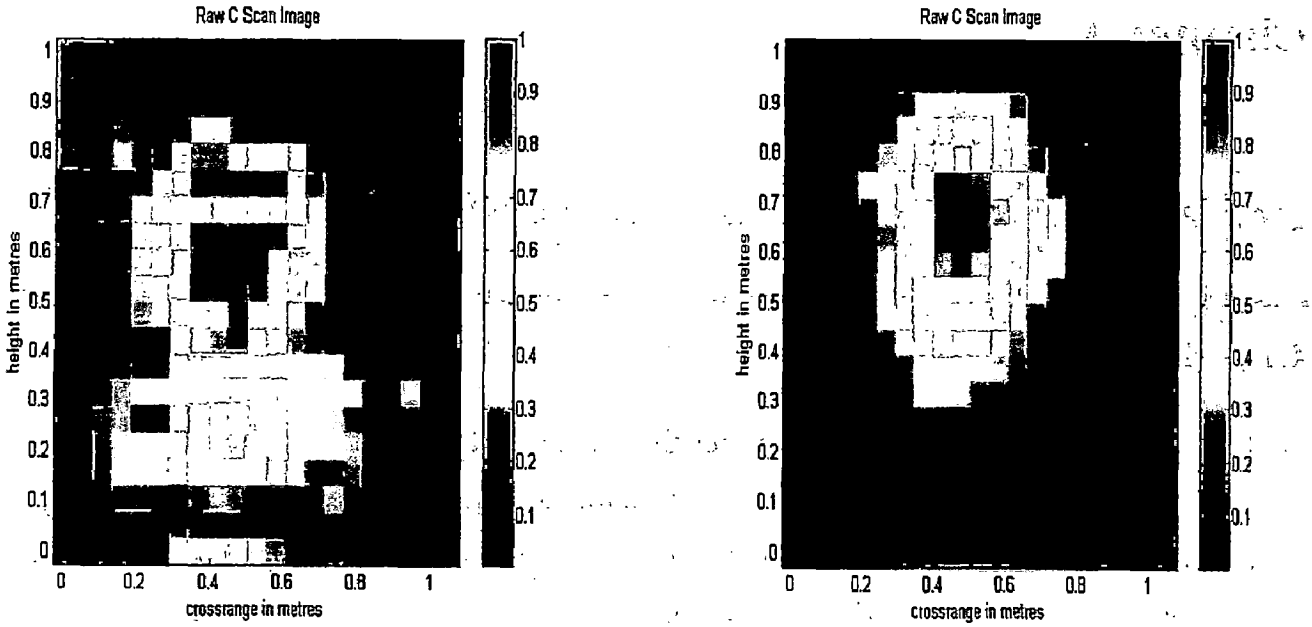

Figure 4.2(a,b): C Scan images for Metallic sheet Parallel to wall

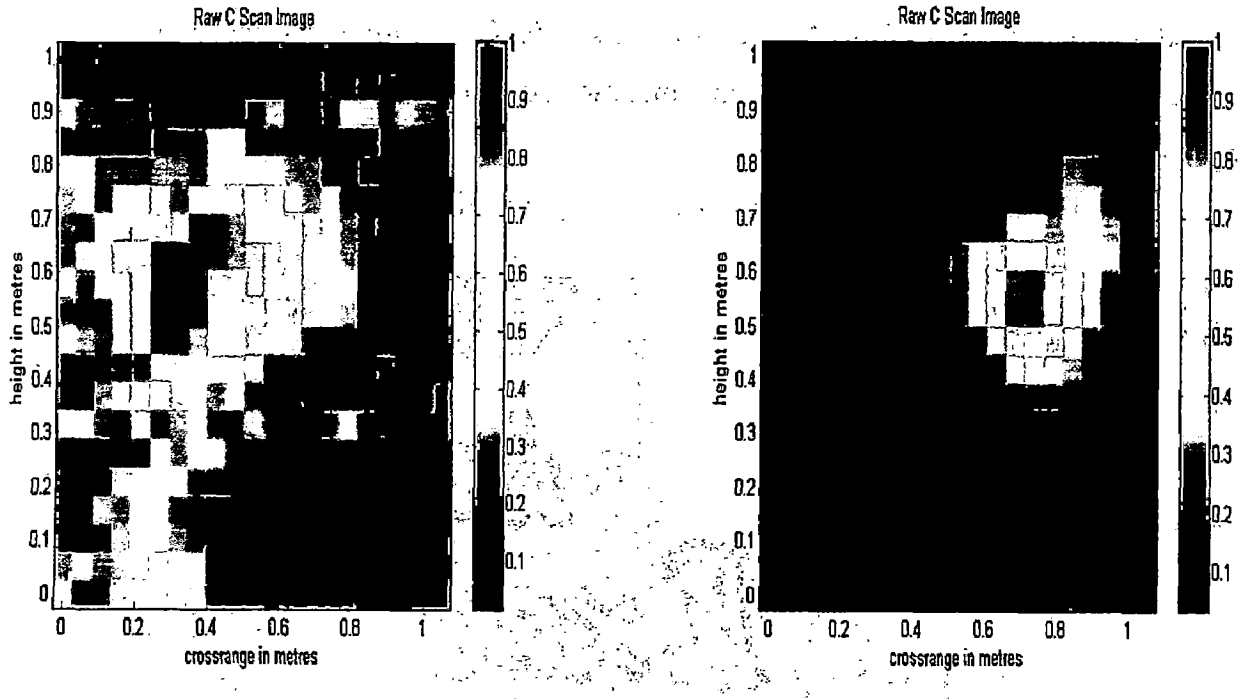

Figure 4.3(a,b): C Scan images for 10 degree oriented target

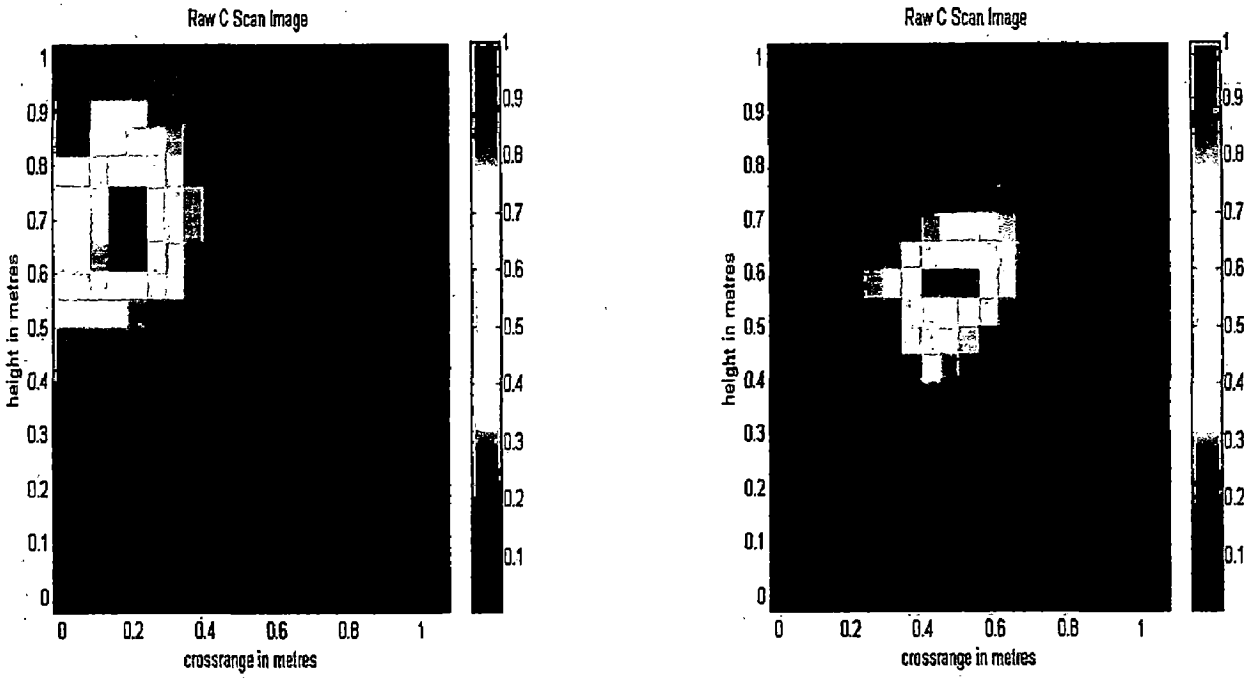

Figure 4.4(a,b): C Scan images for 20 degree oriented target

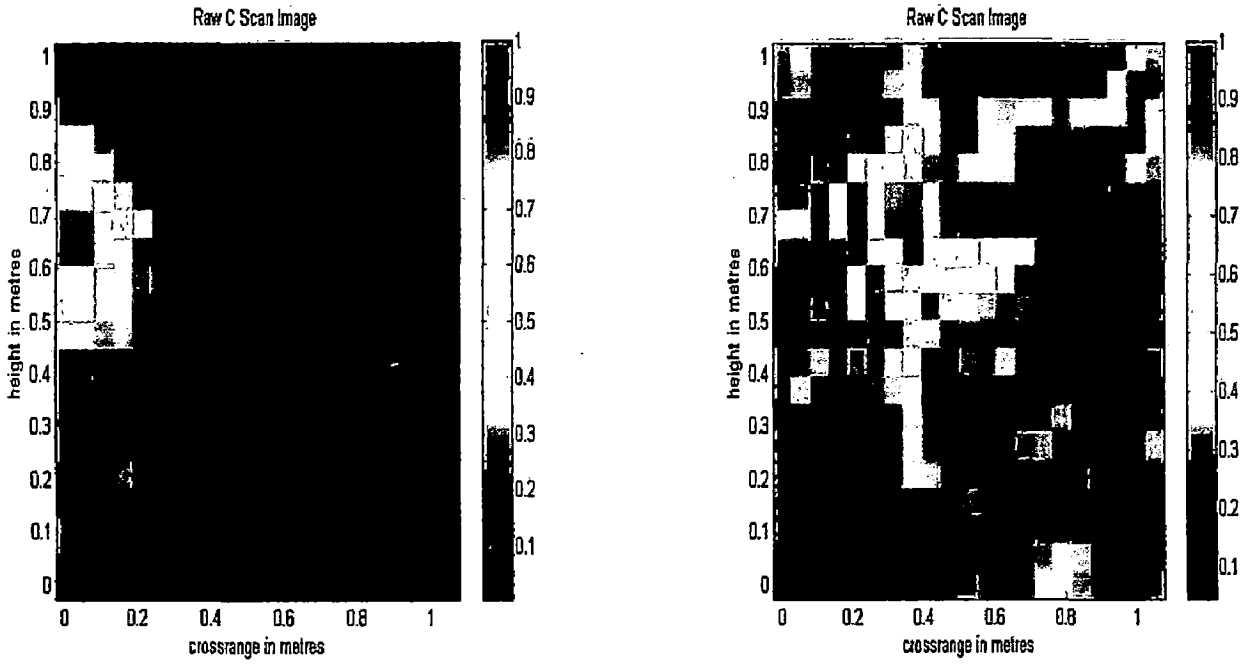

Figure 4.5(a,b): C Scan images for 30 Degree Oriented target

In Figure 4.2 shape detection is very good for circular plate target whether the B Scan data is collected in monostatic mode or bistatic mode and shapes are also of comparable. One can clearly see that the lateral extent of the plate is 0.3 to 0.7 m with center at 0.5 m in both cases. Hence both are equally good as far as shape detection is concerned, but amplitude of reflection is good in monostatic mode as stand does not appear in its image. As the angle of orientation increases from 0 to 10 degree, the center of circle shifts to left and occurs at 0.4 m (with span 0.4 m to 0.6 m) as shown in Figure 4.3 (a). In Figure 4.4(a) i.e. 20 degree tilt and 4.5(a) the center of circle is at 0.2 m (span 0 to 0.4m) and 0 m (-0.2 m to 0.2 m) respectively. This shift is clearly due to orientation of target. Talking about Figures 4.3(b), 4.4(b), the shape distorts more and more and its span in crossrange direction is far less than the expected span and in Figure 4.5(b), it is even hard to indentify the shape. On a conclusive note oriented target detection by using antenna in bistatic mode produces better results when compared to monostatic case. Shift in target location limits the orientation of target. In our experiment up to 30 degree orientation target was detected fine but detected shape starts to distort with further orientation.

4.2. Real Time Moving Target Detection

4.2.1. Target moving in Downrange Direction

(a) Metallic Target

Real time Movement of metallic target behind the wall in downrange direction was successfully detected. Time domain response is generated by following the procedure mentioned in section 3.4. Target was moved in the direction of antenna's main lobe maxima. Snapshots of moving target plots were taken at downrange distance 30cm, 60cm, 1m, 1.5m and 2m. One can notice 4 or 5 peaks which are due to cable –antenna connection, antenna-air reflection, reflection due to walls and target response from left to right respectively. The rightmost peak is due to target which is highlighted by putting a marker sign on it. EM radiation travels slower in wall, so the downrange distance is greater than expected. Though considering 1m mark as wall boundary; the distances of detected target peaks from this mark are roughly same as actual. The peak corresponding to target flattens down as downrange distance increases as reflection from target becomes weaker and weaker. Snapshots of the moving target taken at 1s, 4s, 7s, 9s, shows their respective spatial domain response in Figures 4.6, 4.8, 4.9, 4.10.

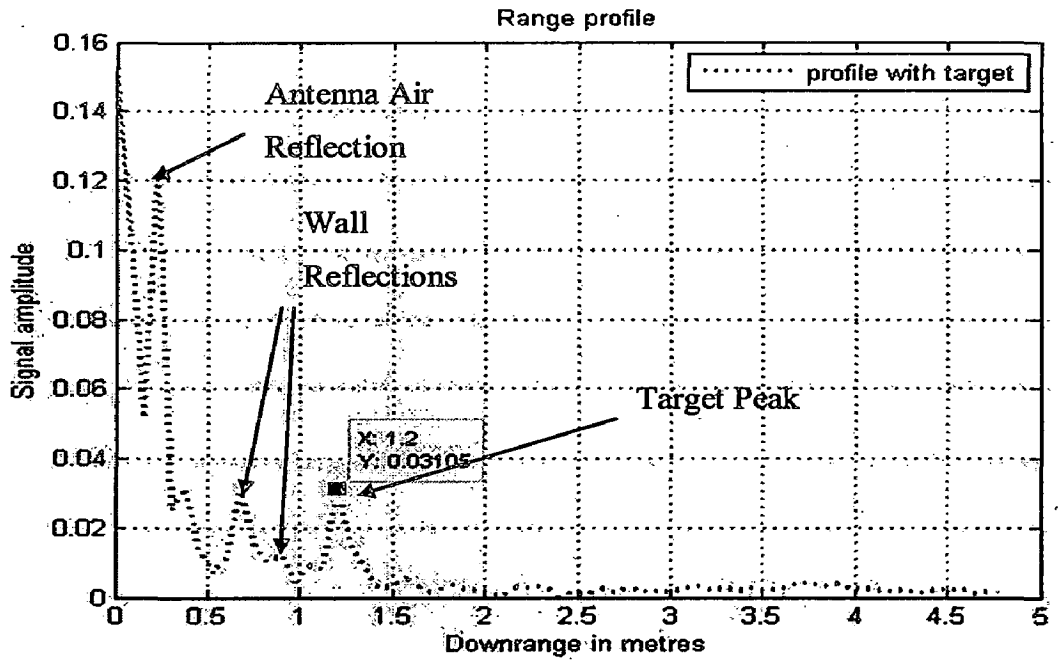

Figure 4.6: Circular plate 30 cm away from wall

One can further generate background subtracted image in which peaks due to antenna air interface, wall reflection disappears and only peak due to target remains as shown in figure 4.6.

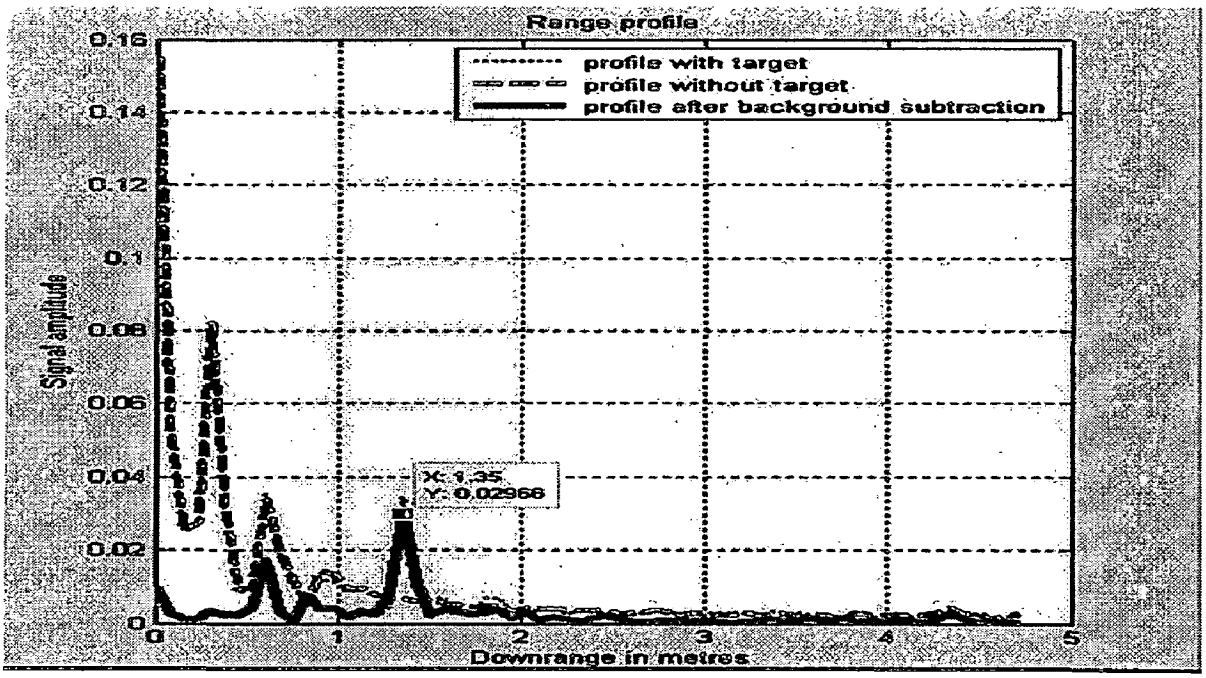

Figure 4.7: Plot of target at 30 cm with background subtraction

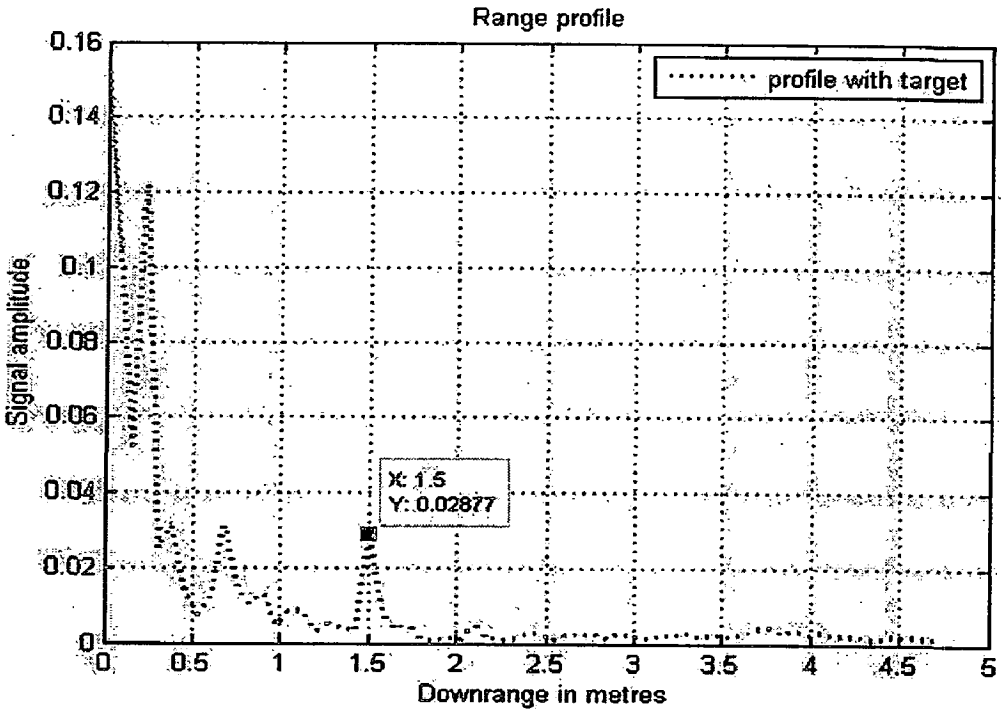

Figure 4.8: Circular plate 60 cm away from wall

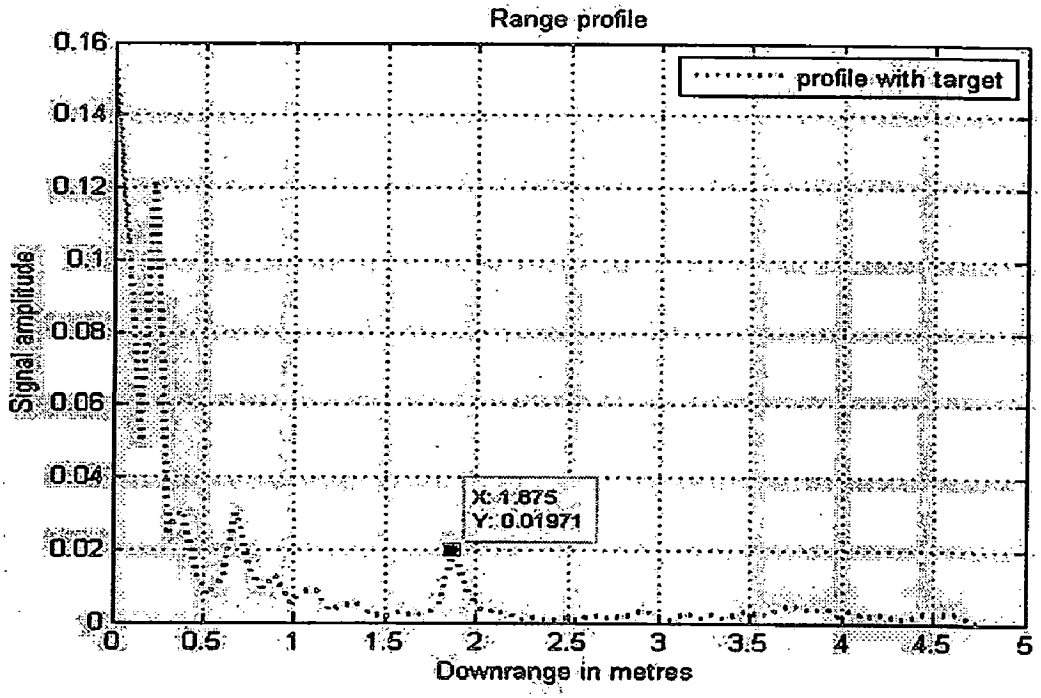

Figure 4.9: Circular plate 1 m away from wall

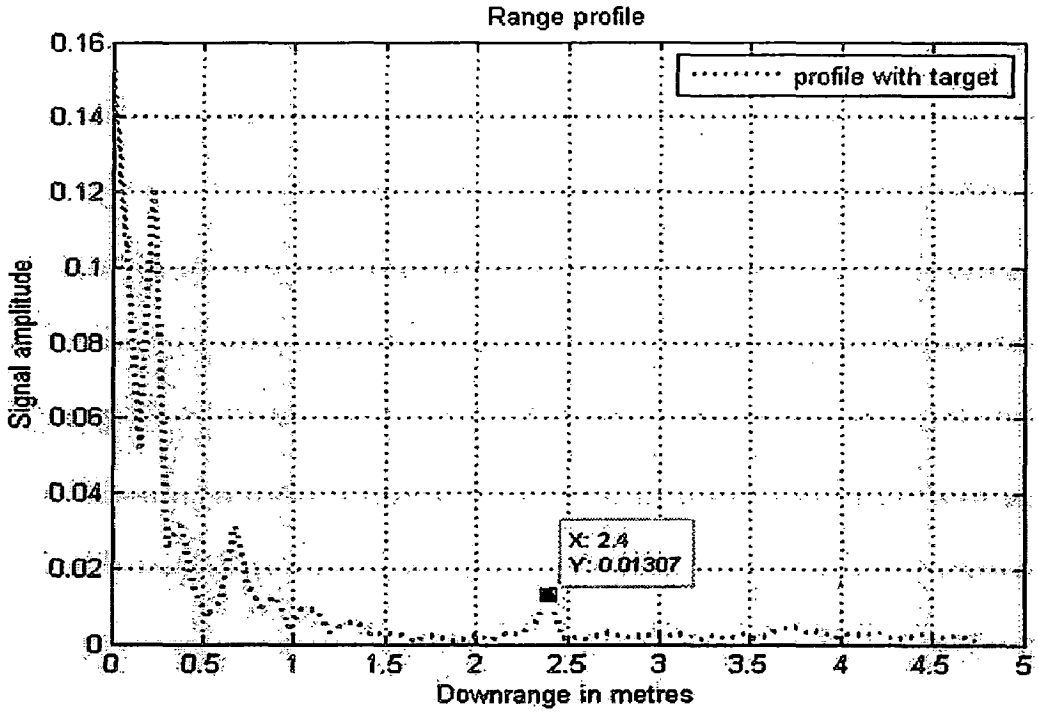

Figure 4.10: Circular plate 1.5 m away from wall

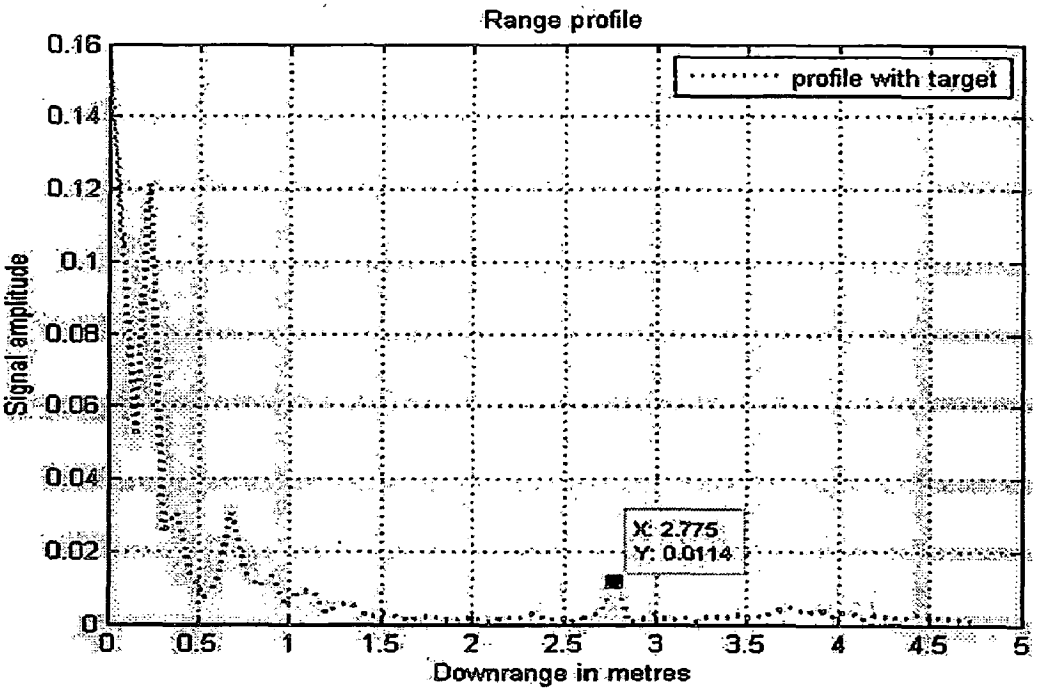

Figure 4.11: Circular plate 1.5 m away from wall

From the snapshots at different times the data we get is

At time t = 1s distance from antenna = 1.2 m

At time t = 4s distance from antenna = 1.875 m

At time t = 7s distance from antenna = 2.4 m

At time t = 9s distance from antenna = 2.8 m

So, roughly the velocity of the target with first two reading is equal to (1.87-1.3)/3 = 0.19 m/s

The velocity of the target with 2nd and 3rd reading is equal to (2.4-1.875)/2 = 0.175 m/s

Hence the velocities are comparable with actual velocity. Further one can judge the attenuation is about 1.5dB/m from above pictures.

(b) Human

Reflection response due to human walking at rate 2 steps/sec is very faint and background subtraction need to be applied. But background subtraction in spatial domain is not perfect which leads to negative signal amplitudes in overall image. So, negative value filtering was applied to the background subtracted plot. Figures 4.12, 4.13, 4.14, 4.15 and 4.16 for human distance 30 cm, 60 cm, 1m, 1.5m and 2m from wall respectively show the amplitude attenuation of signal with increasing downrange distance. Highlighted peak is target and rest small peaks are noise components.

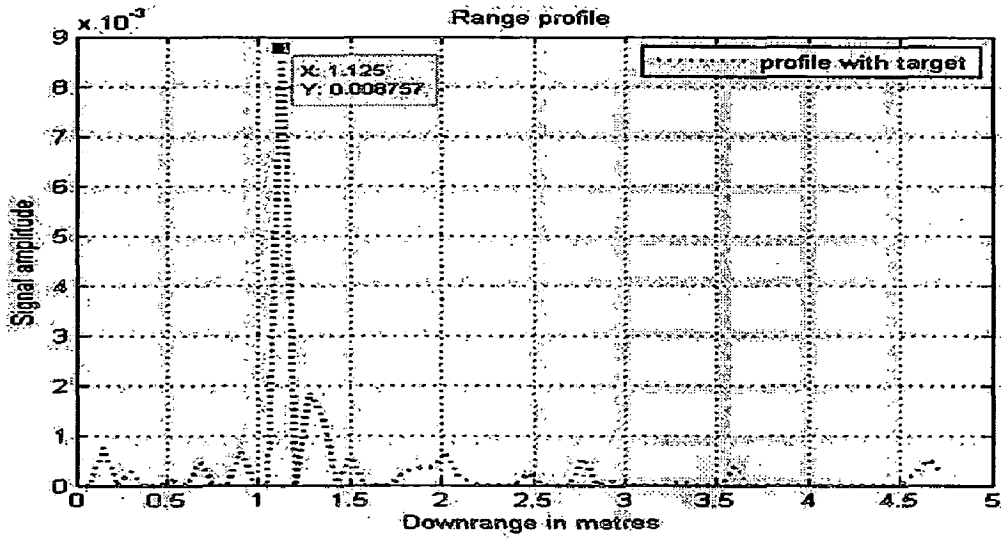

Figure 4.12: Human 30 cm away from wall

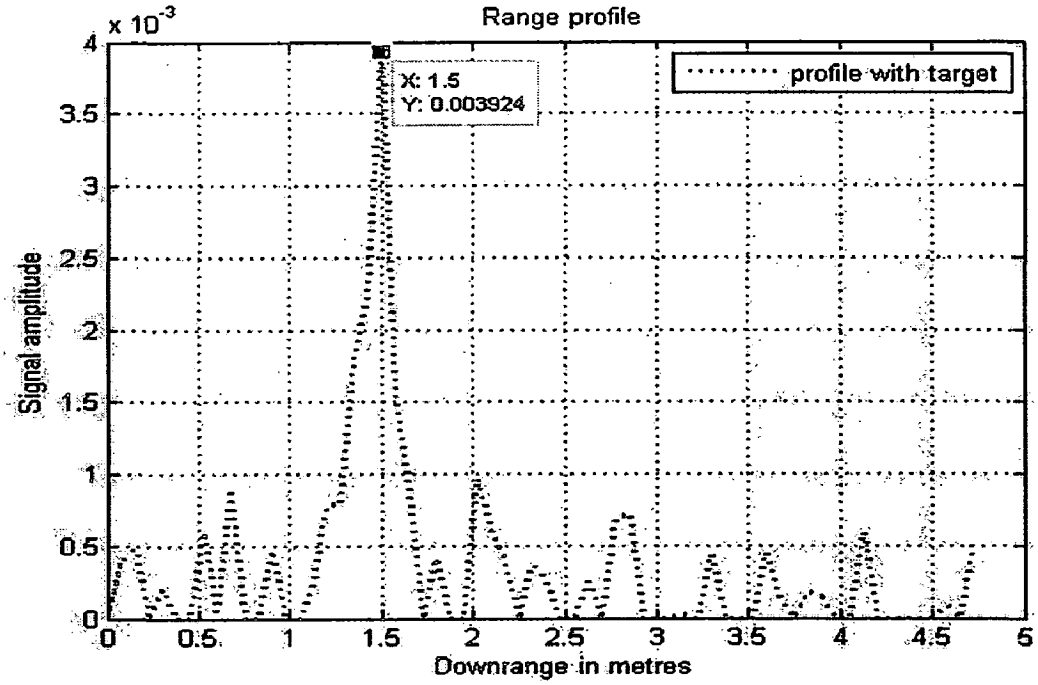

Figure 4.13: Human 60 cm away from wall

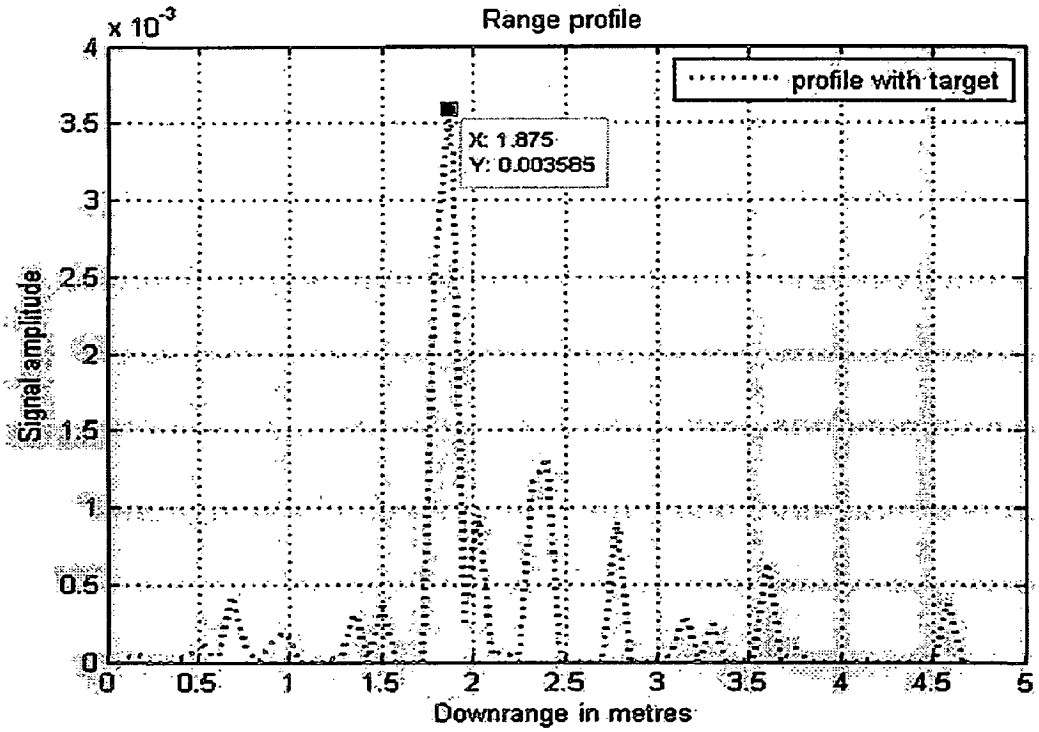

Figure 4.14: Human 1m away from wall

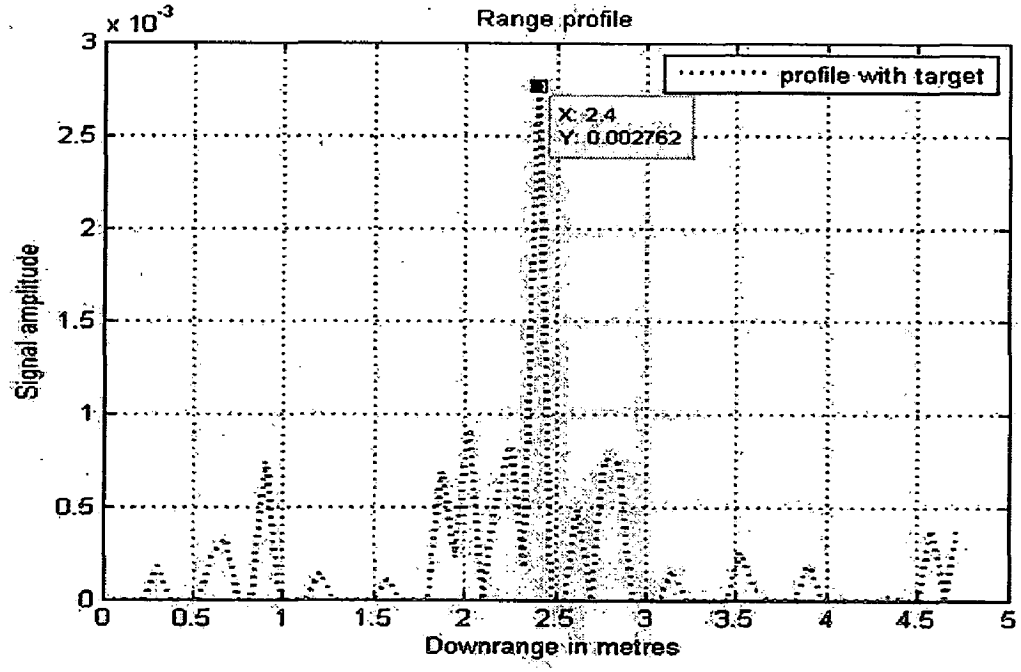

Figure 4.15: Human 1 m away from wall

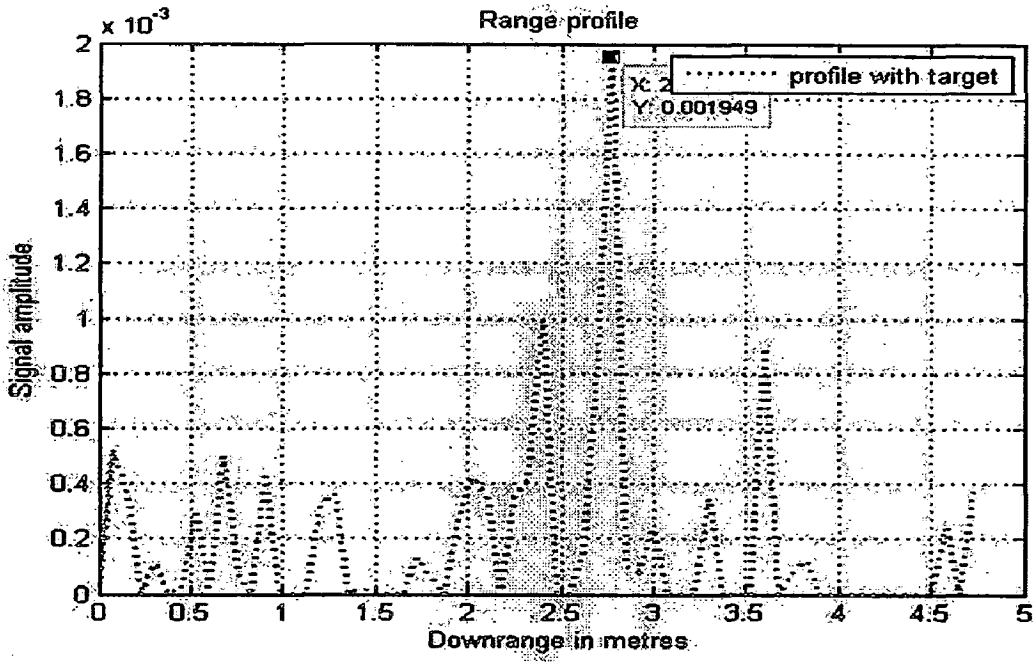

Figure 4.16: Human 2 m away from wall

There were 5 transitions in 3 seconds in the target peak as human moved from 30 cm to 2m on the other side of wall. This gave us information that human is taking a step of size 35 cm. It can be concluded that the human was moving at the rate 2 steps/ sec from distance 30 cm to 2m from wall. Initially when human moves from 30cm mark to 60m mark attenuation in signal amplitude was very high. While moving further; attenuation was more or less steady (2.2 dB/m).

4.2.2. Target moving in Crossrange Direction

(a) Metallic Plate

In this experiment the circular metallic plate of radius 8 inches was moved parallel to the surface of wall at a constant downrange distance of 60 cm. The motion of circular plate was in crossrange direction only. Iterative time domain response was generated using algorithm discussed in section 3.4. It was observed that the target reflection or signal amplitude is the maximum when the target is in front of direction of maximum radiation of antenna. The signal peak diminishes very fast as plate moves away from the wall. Even after slightly more than 60 cm shift of plate away from maxima; the signal response becomes negligible. Snapshots of the moving target taken at 0cm, 20cm, 40cm, 60 cm away from direction of maximum radiation; shows their respective spatial domain response in Figures 4.17, 4.18, 4.19,4.20 respectively..

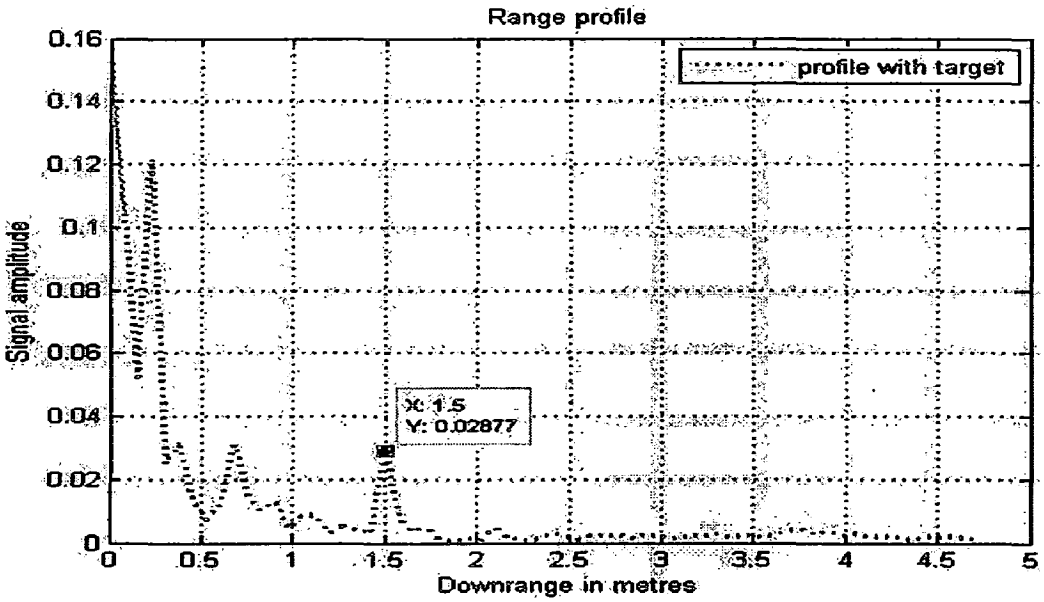

Figure 4.17: Metallic plate (in front on antenna) 60 cm from wall.

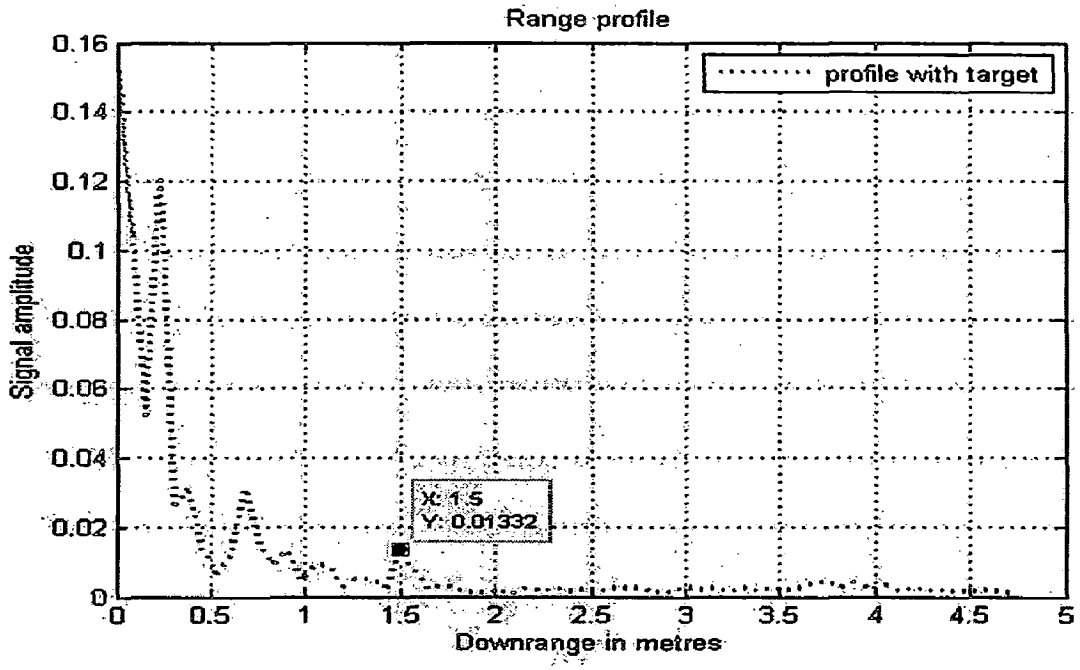

Figure 4.18: Metallic plate (crossrange 20 cm from antenna) 60 cm from wall.

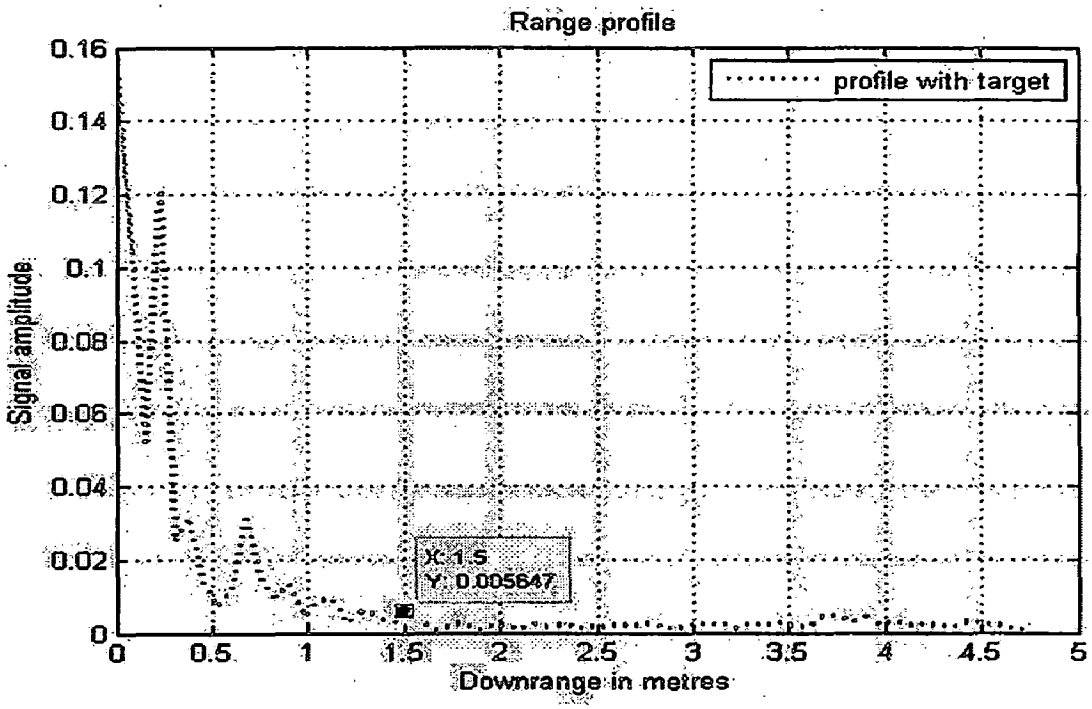

Figure 4.19: Metallic plate (crossrange 40 cm from antenna) 60 cm from wall.

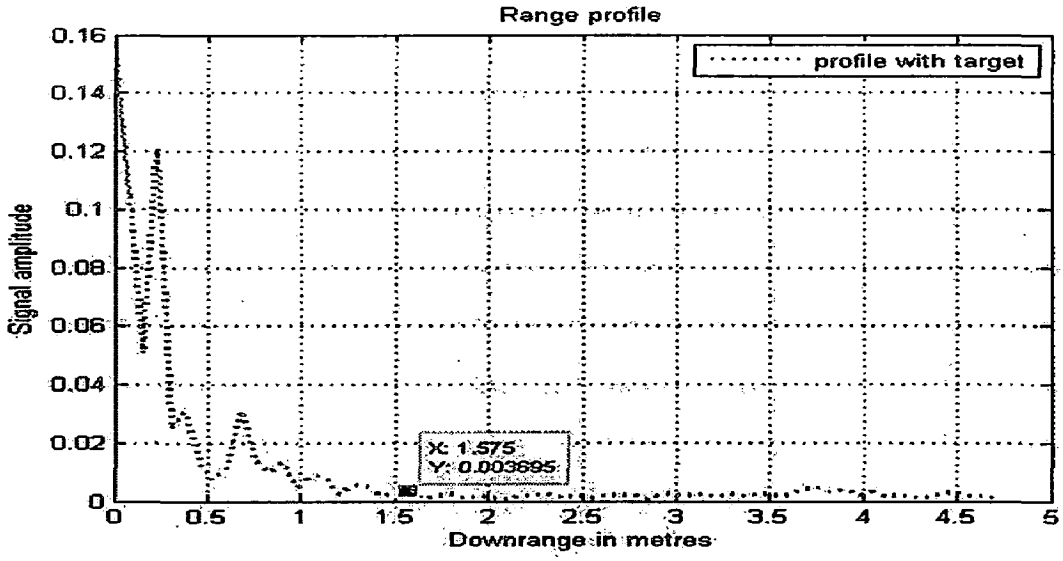

Figure 4.20: Metallic plate (crossrange 60 cm from antenna) 60 cm from wall.

When target moves to and fro around direction of maximum radiation these range profiles are repeated but the range of target remains almost same. From the frequency of repetition of the peak value amplitude velocity of the target moving in crossrange direction can be estimated. For this case the whole waveform repeats after 6 s; that implies target is in front of maxima of beam after every 6s. Looking at the signal amplitude we got:

Signal amplitude in front of antenna's maximum radiation direction = 0.02877
Signal amplitude when target was 20cm away from antenna in crossrange = 0.01332
Signal amplitude when target was 40cm away from antenna in crossrange = 0.00565
Signal amplitude when target was 60cm away from antenna in crossrange = 0.00369
Moving further there is not a significant target response due to movement far away from main lobe maxima. Also incident radiation gets reflected away from antenna and can only be received if antenna array is used. It is clear that signal amplitude after successive 20 cm advance away from antenna in crossrange direction is almost halved. So, the attenuation in signal is roughly 3dB/20cm or 15db/m in crossrange direction.

(b) Human

Target response of walking human across crossrange direction with constant distance from wall 60 cm in similar fashion as metallic plate movement is also recorded.

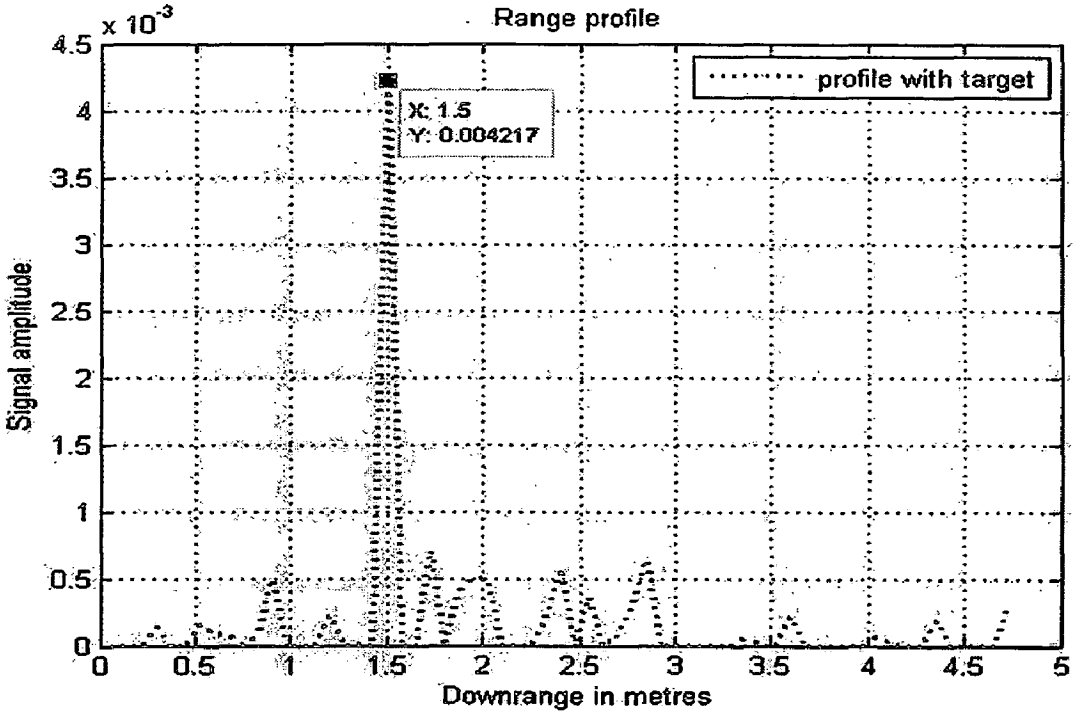

Figure 4.21: Human (in front on antenna) 60 cm from wall.

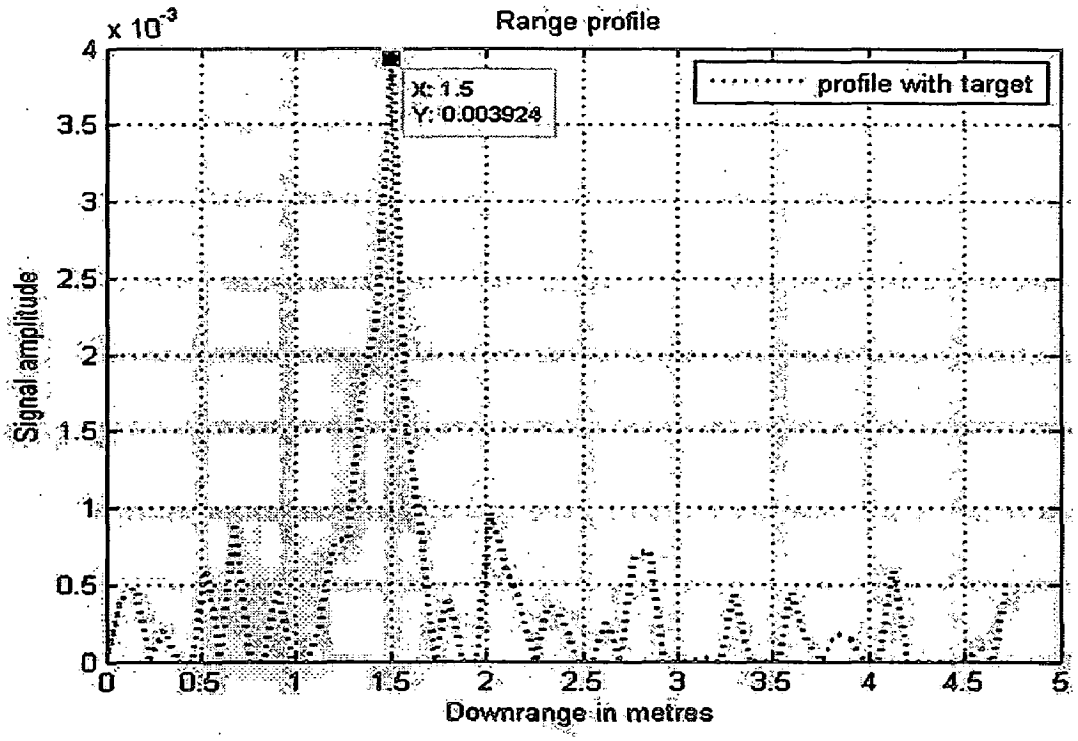

Figure 4.22: Human (Crossrange 20 cm from antenna) 60 cm from wall.

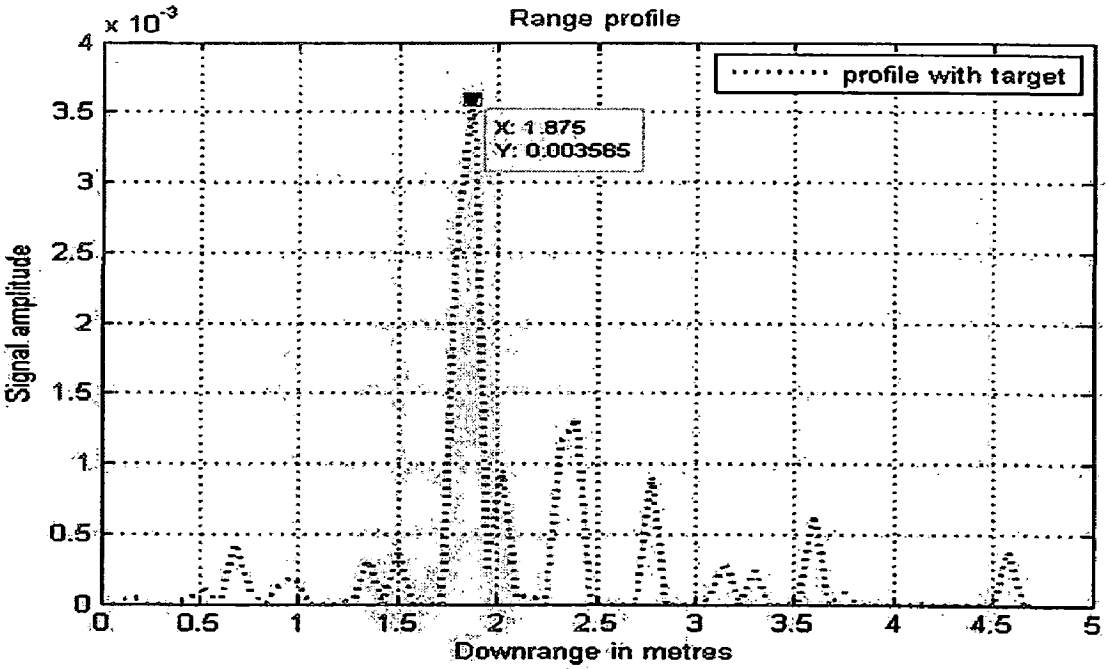

Figure 4.23: Human (Crossrange 40 cm from antenna) 60 cm from wall.

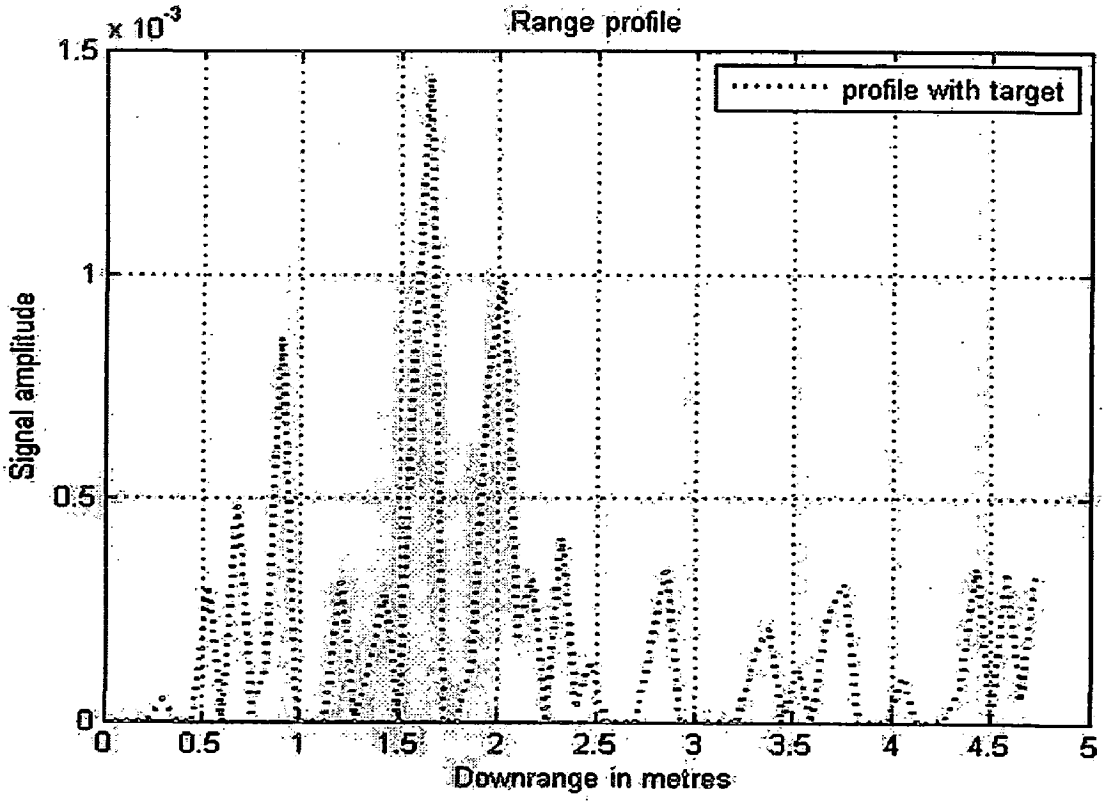

Figure 4.24: Human (Crossrange 60 cm from antenna) 60 cm from wall.

From Figures 4.21, 4.22, 4.23 it is evident that the signal amplitude of human doesn't change significantly with crossrange movement. It remains constant around 0.004. This is due to the fact that human body is not a good reflector of radiation as metal sheet. It reflects the good percentage of radiation back to the direction of incidence i.e. antenna unlike metal sheet which reflects majority of radiation away from antenna if angle of incidence is greater than 10 degree. So amplitude of reflected signal doesn't change. However with crossrange movement, after some point human starts getting out of antenna's main lobe; leading to poor reflection as clear in Figure 4.24.

4.2.3. Detection of standing and standing human

Spatial domain response of the sitting and standing human in front of antenna beam at distance 60 cm away from the wall was taken. Figure 4.25 corresponds to the response of standing human while Figure 4.26 corresponds to response of sitting human.

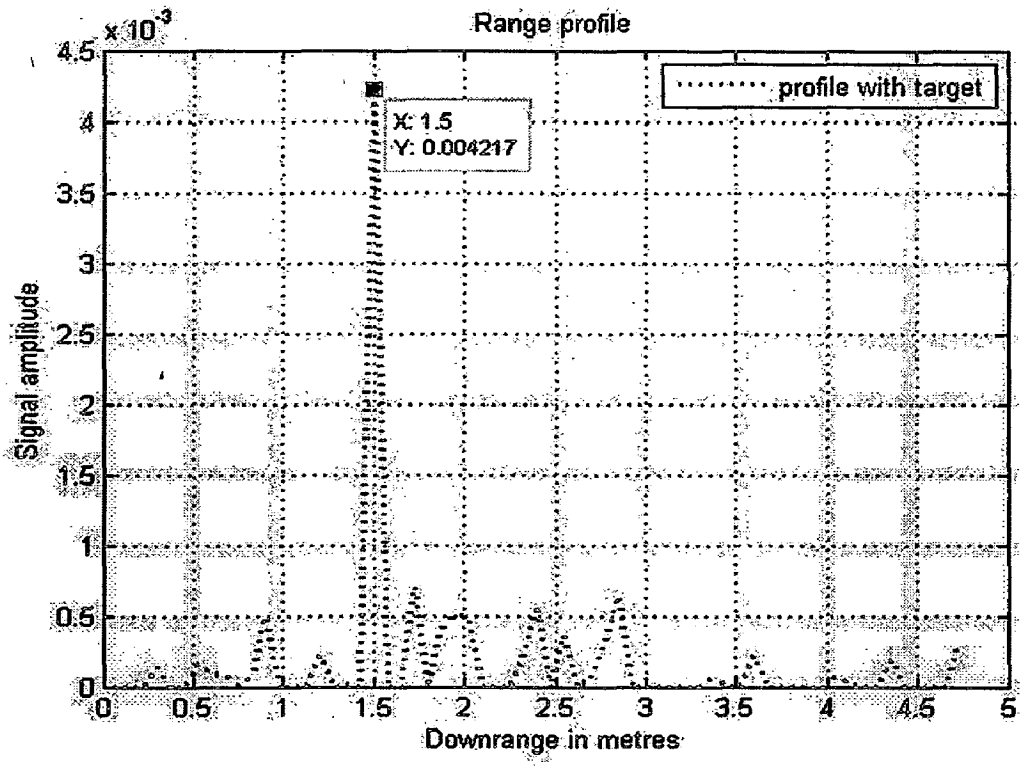

Figure 4.25: Standing human 60 cm away from wall

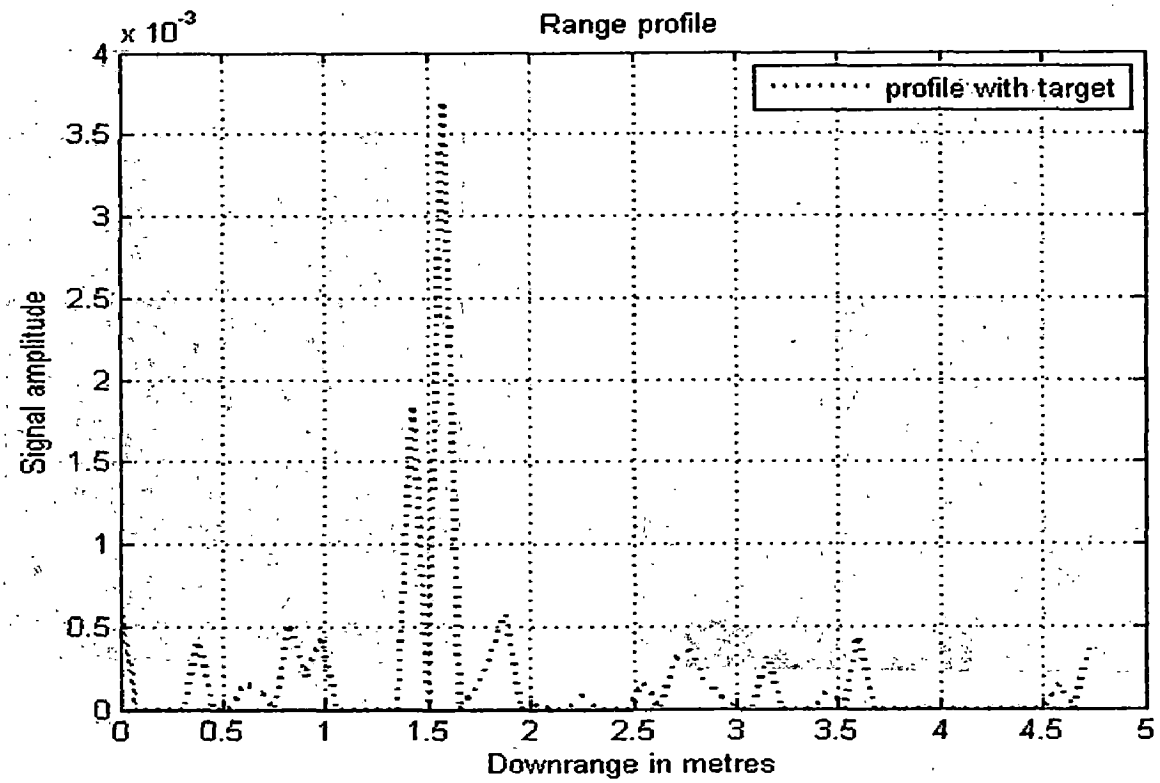

Figure 4.26: Sitting human 60 cm away from wall.

Standing and sitting humans can be distinguished on the basis of singnal amplitude. Signal amplitude on standing human is roughly 20% greater than sitting human. Also the sitting human is located slightly farther in downrange in comparison of standing human reason being the greater travelling path for human sitting at ground level.

4.3. Human Detection & Imaging

A full C scan of human shown in Figure 4.27 (a) is performed. Scanning roughly starts from knee level of human. On application of image generation algorithm there is headless human as shown in Figure 4.27 (c) that means no response corresponding to Human head while arm is detected. While on application of ICA algorithm and selection of appropriate range index on the data corresponding to height levels belonging to human head, it become visible as shown in Figure 4.27 (b) and 4.27 (c). However human's span is more than expected in cross range. Possible reasons behind this are the uneven scattering of human body. The antenna also gets the reflection due to the side part of human body. So effective area from which antenna receives reflection increases. *Distance of antenna from wall = 40 cm, wall to target = 30 cm.*

(a)

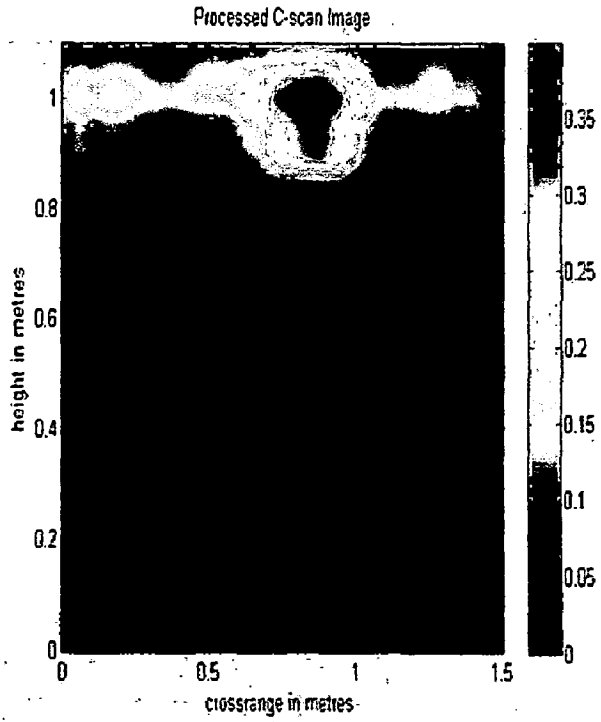

(b)

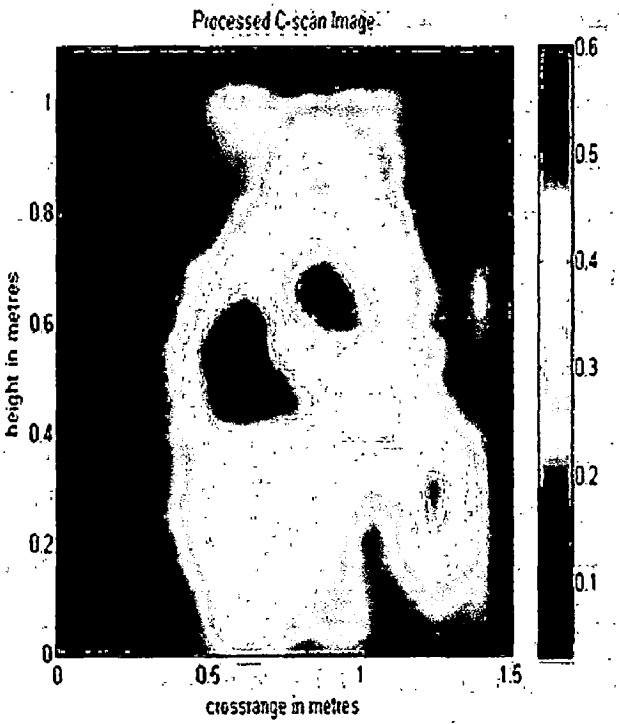

(c)

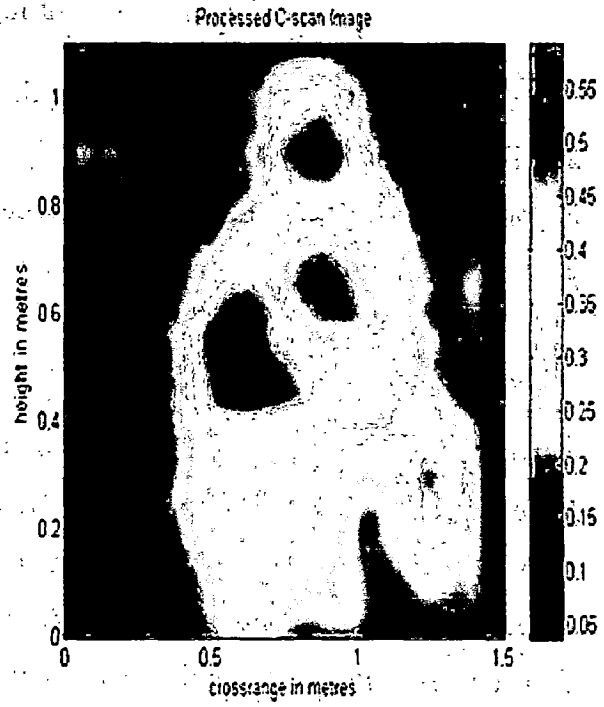

(d)

Figure 4..27: (a) Human (b) Head detected by ICA (c) Raw C Scan image (d) Sum Image of (b) & (c)

4.4. Human Heart Beat Detection

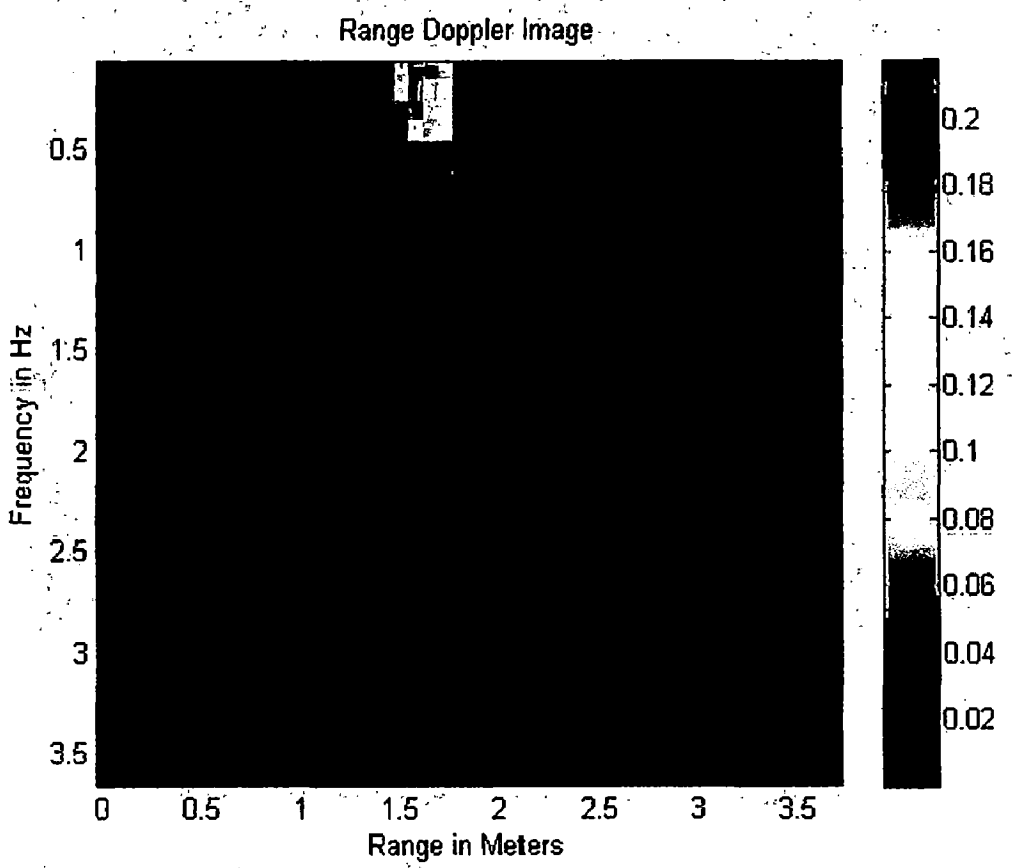

Figure 4.28: Range Doppler Image without MTI for human at 70 cm

Simple Range Doppler Image: The experiment was conducted to detect the heart beat of human standing 70 cm behind the wall. Radar scanning system was assembled and antenna was set at height such that the radiation illuminates the thorax region of the human. One sweep of SFCW radar with 889 points consists of 40 milliseconds. 250 such sweeps were repeated; hence antenna radiates for 10 s. Complex frequency domain was collected on which Range Doppler processing (IFFT on rows and FFT on columns of complex frequency data) was done as discussed in section 3.5.4. Due to presence of human target a column with high intensity values appear in Range Doppler plot. But frequency values corresponding to heart beat i.e. 1.2 to 2 Hz are not highlighted due to peak response at 0^{th} frequency. This is due to stationary targets and wall, whose frequencies of movement are zero, but are high reflection amplitude source.

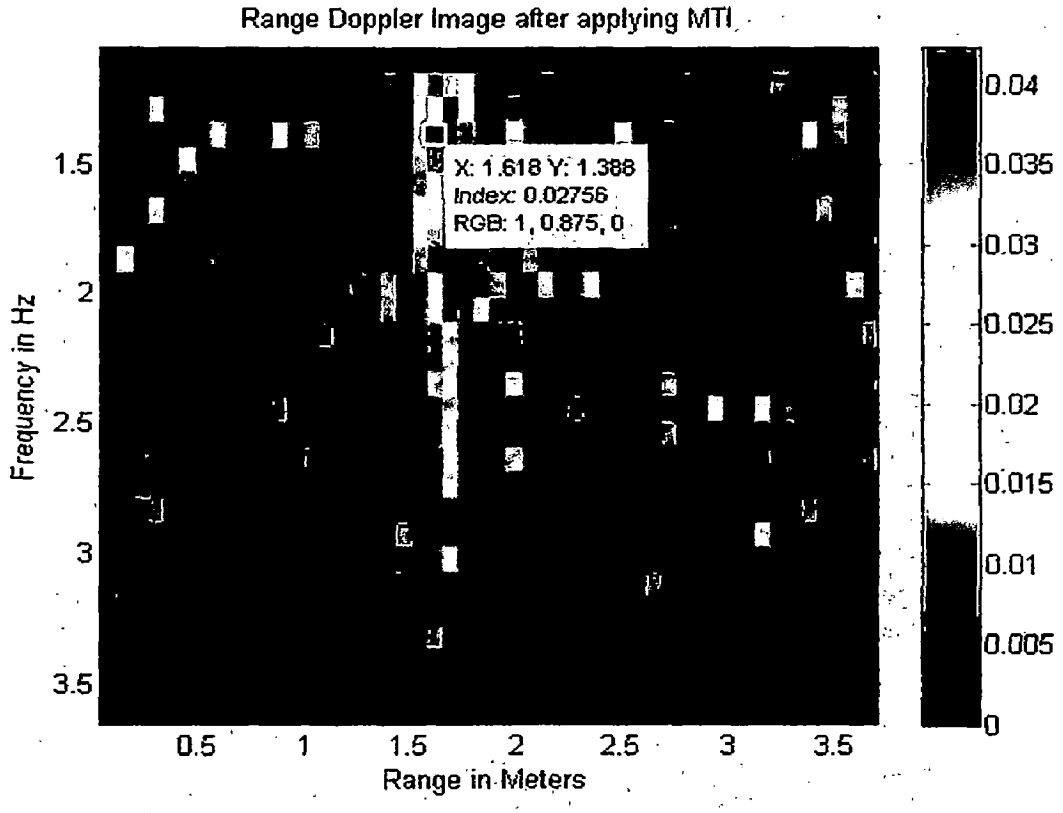

Figure 4.29: Range Doppler Image with MTI for the same

Range Doppler Image after application of MTI: With application of recursive moving target indicator filter with K value 0.85, stationary response this is filtered out and we can see frequency peak at 1.5 Hz in Figure 4.29. One can also notice the increased amplitude of the heart beat frequency. This filter is applied after application of IFFT on rows and before application of FFT on the columns of complex frequency domain data. This plotted response is capable of showing frequencies from 1 to 3.5 Hz within downrange 3.5m.

Range Doppler Image for non living things and background: Consider the case when there is no human but only potential metallic targets are there. One can notice that there is no single column of high intensity in 1 Hz to 2 Hz frequency range values as it was observed in Figures 4.28 and 4.29. Then was no unique high intensity region as shown in Figure 4.30 even if the metallic target is just 30 cm away from the wall. Similarly no unique peak value in expected range occurs, as shown in Figure 4.31; for the case of no target (background only). From these Figures one can conclude the absence of the human on the basis of random frequency map. Very little chance of false heart beat detection is there.

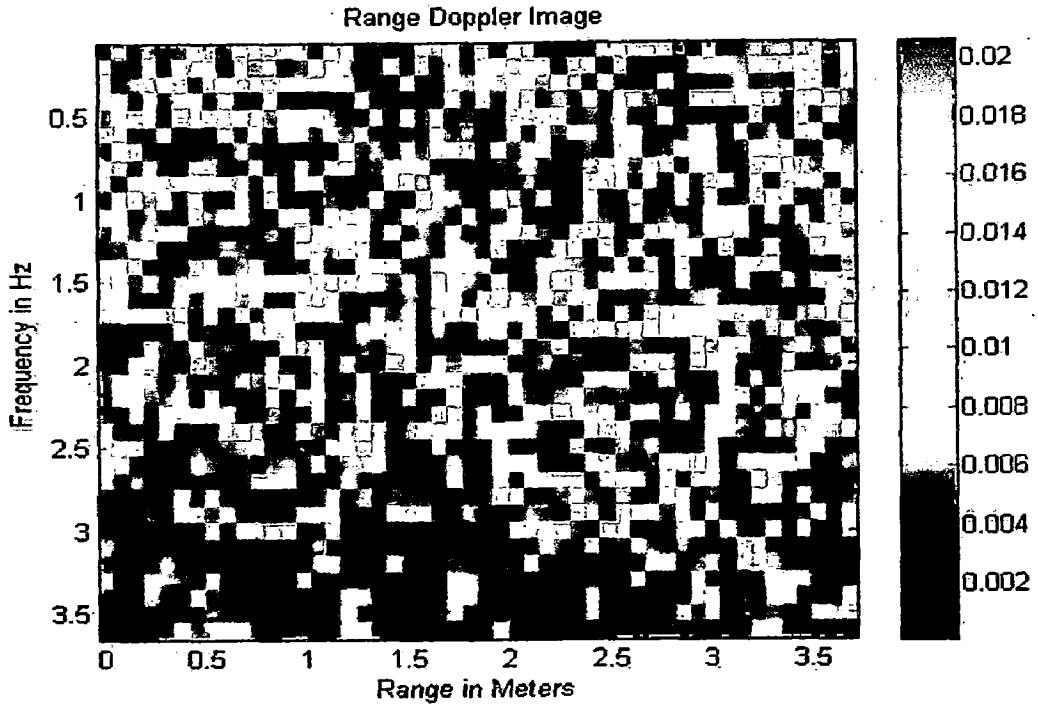

Figure 4.30: Range Doppler Image for metallic sheet at 30 cm from the wall.

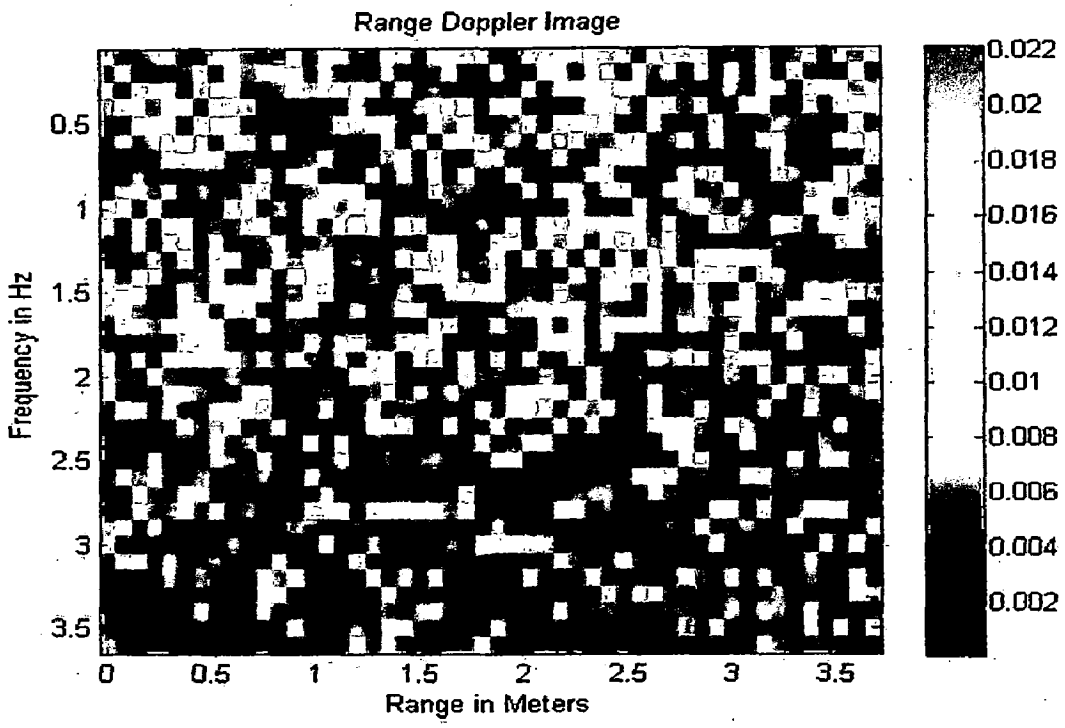

Figure 4.31: Range Doppler Image for Background

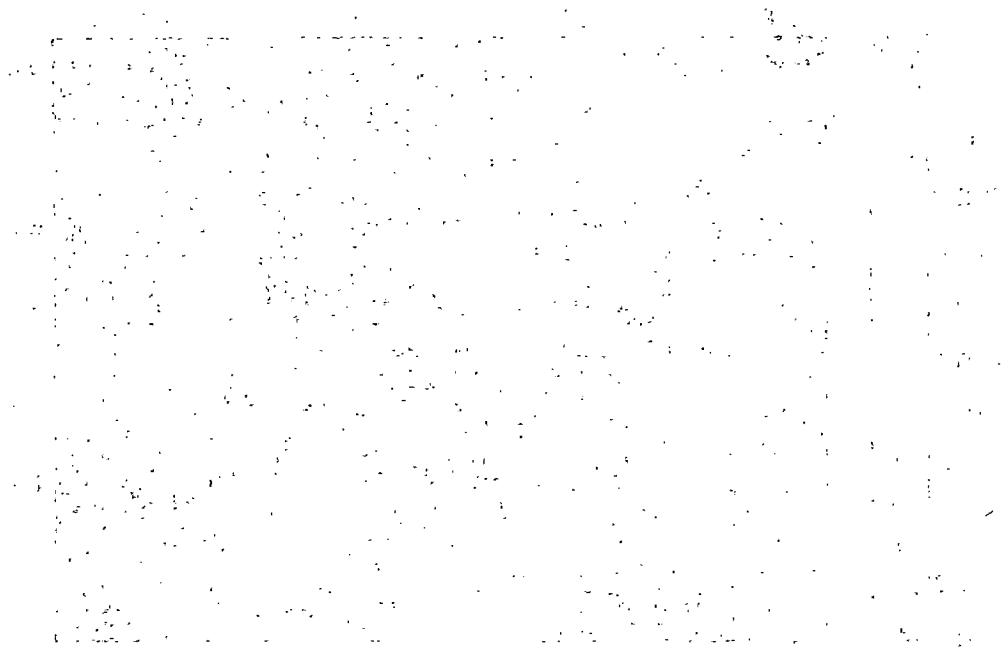

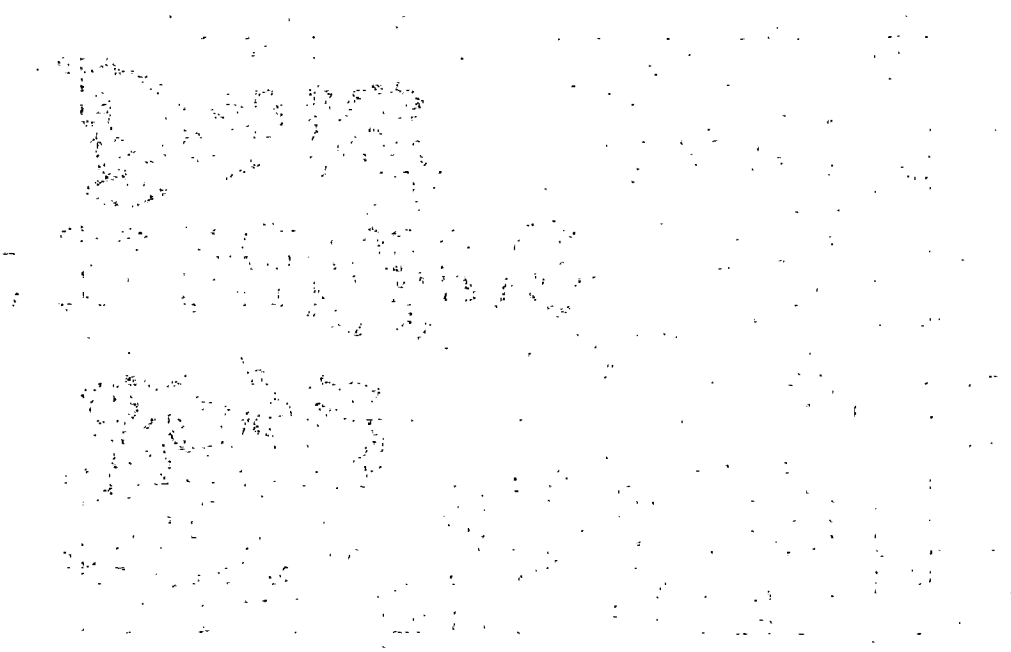

Chapter 5

Conclusion & Future Work

Metallic and non–metallic targets of different shape and dielectric constant are successfully detected by running B Scan. Metallic targets show good response due to their good reflection properties; while running B Scan for low dielectric target like Teflon results in faint response in corresponding raw image. Singular Value Decomposition (SVD) and Independent Component Analysis (ICA) have been applied for clutter reduction. Clutter reduction techniques make the targets more visible and background clutter is visibly reduced. However, for detection of a low dielectric target, like Teflon, SVD does not provide satisfactory results and ICA is able to make target detection possible. Oriented target detection was one of this project which was being worked on. A comparative study on the circular plate target detection by antenna in monostatic as well as in bistatic mode is done. It was observed that antenna in bistatic mode gives fine results as far as shape detection is concerned. But a shift is observed in circular region in C scan image from the expected location. This is due to orientation that incident radiation is received as far away as the angle increases. Antenna in monostatic mode fails to show the exact shape and at 30 degree it gives unacceptable distorted shape.

Real time Movement of metallic target behind the wall is successfully detected; however response corresponding to human is very faint but was improved using background subtraction followed by negative filtering. The peak corresponding to target flattens down as distance of target from antenna increases as reflection from target becomes weaker and weaker. Crossrange motion of human is detected but in this case amplitude of signal faces severe attenuation as target moves away from main lobe maxima. In case C Scan of the human is taken and it is observed that the rest of body is detected apart from head. With the application of ICA algorithm on levels corresponding to head and fusion of two images the whole human was detected. Still the human's span it the cross range is little more than expected due to uneven scattering by human body. Human heart beat is the chief factor which distinguishes human from human mock-ups. Range Doppler processing on data obtained corresponding to 250 frequency sweeps and 889

range bins. The distance of human from antenna and is found to be accurate while the frequency of heart is diminished due to dominant 0^{th} frequency corresponding to stationary targets like walls, still parts of human body and other surrounding. However on application of MTI i.e. moving target indicator and appropriate selection of its parameters human heart beat becomes visible in the acceptable range.

Shape of 2-dimentional objects like circle, square, triangle is identified correctly till now even for low dielectric constant materials like Teflon. Detection of 3 dimensional objects like cylinder, sphere, cube and other various shapes is the gray area where a little research has been done till now like Debes worked in his thesis on superquadrics based model to identify both geometrical (shape) and statistical features. Detection of metallic 3 D objects is still a challenge as from single wall detection of sphere is not feasible and requires more vantage points. In this thesis targets oriented about vertical axis only are detected, so targets oriented about horizontal axis should be detected. Data processing should be made efficient so as to get shape information of small targets lying in antenna swath by running a single B Scan at appropriate height. Keeping the detection of human heart beat in mind, research on human motion activities, like hand movement, walking: should be done.

References

[1] D.D. Ferris Jr. and N.C. Currie, "A survey of current technologies for through-the-wall surveillance (TWS)," In Proceedings of SPIE, vol. 3375, pp. 62-72, 1998.

[2] E.J. Baranoski, "Through-wall imaging: Historical perspective and future directions," Journal of Franklin Institute, vol. 345, pp. 556–569, 2008.

[3] Johnson, J.T., Demir, M.A. and Majurec, N., 2009, "Through-wall sensing with multi-frequency microwave radiometry: a proof of concept demonstration". IEEE Transactions on Geoscience and Remote Sensing, 47, pp. 1281–1288.

[4] Lizuka, K., Freundorfer, A.P., Wu, K.H., Mori, H., Ogura, H. and Nguyen, V., 1999, Step frequency radar. *Journal of Applied Physics*, 56, pp. 2572–2583.

[5] Curie, N. C., 1989, *Radar Reflectivity measurement: Technique and Applications,* (Artech House, Norwood MA).

[6] Shirodkar, S.; Barua, P.; Anuradha, D.; Kuloor, R.; , "Heart-beat detection and ranging through a wall using ultra wide band radar," *Communications and Signal Processing (ICCSP), 2011 International Conference on* , vol., no., pp.579-583, 10-12 Feb. 2011

[7] A. Yarovoy, "Ultra-Wideband Radars for High-Resolution Imaging and Target Classification", In *Proceedings of 4th European Radar Conference*, pp. 1-4, 2007.

[8] A. Langman and M.R. Inggs, "A 1-2 GHz SFCW radar for landmine detection," In *Proceedings of the 1998 South Asian Symposium on Communications And Signal Processing*, pp. 453-454, 1998.

[9] I.L. Morrow and P.V. Genderen, "Effective imaging of buried dielectric objects," *IEEE Transactions on Geoscience and Remote Sensing,* vol. 40, pp. 943-949, 2002.

[10] D. J. Taylor, Introduction to Ultra-wideband Radar Systems, CRC press, 1995.

[11] Dehmollaian, M. and Sarabandi, K., 2008, "Refocusing through building walls using synthetic aperture radar" *IEEE Transactions on Geoscience and Remote Sensing*, 46, pp. 1589–1599.

[12] D. D. Ferris Jr. and N. C. Currie, "*Microwave and millimeter wave systems for wall penetration,*" In *Proceedings of SPIE*, vol. 3375, pp. 269-279, 1998.

[13] FCC Ultra-Wideband Notice of Propose Rule Making (NRPM) 2000, Federal Register, vol. 65, no. 115, 14 June 2000.

[14] Hunt, A.R. and Hogg, R.D., 2002, "A stepped-frequency, CW radar for concealed weapon detection and through the wall surveillance" In *Proceedings of SPIE*, 4708, pp. 99–105.

[15] A. Langman and M.R. Inggs, "A 1-2 GHz SFCW radar for landmine detection," In *Proceedings of the 1998 South Asian Symposium on Communications And Signal Processing*, pp. 453-454, 1998.

[16] Hunt, A.R., 2009, "Use of a frequency hopping radar for imaging and motion detection through walls". *IEEE Transactions on Geoscience and Remote Sensing*, 47, pp. 1402–1408.

[17] Frazer, L. M., 1996, "Surveillance through walls and other opaque materials" In *Proceedings of the IEEE National Radar Conference,* 13–16 May 1996, Michigen USA, pp. 27–31.

[18] Staderini, E.M.; "UWB radars in medicine" *Aerospace and Electronic Systems Magazine, IEEE*, Volume 17, Issue I, Jan. 2002 Page(s) 13 -18.

[19] Gabriel, C.; "Compilation of the Dielectric Properties of Body Tissues at RF and Microwave Frequencies" *Physics Department, King's College London, London WC2R2LS, UK; Armstrong Laboratory (AFMC)*, Occupational and Environmental Health Directorate, Radiofrequency Radiation Division. Report: AOE-TR- 1996-0037

[20] P.K. Verma, A.N. Gaikwad, D. Singh, and M.J. Nigam, "Analysis of clutter reduction techniques for through wall imaging in UWB range," *Progress In Electromagnetics Research B*, vol. 17, pp. 29-48, 2009.

[21] Chang, Y.J.; "The NPAC Visible Human Viewer:" *Data from Visible Human Project* Syracuse University, New York.

[22] Zhou Yong-shun, Kong Ling-jiang, Cui Guo-long, Yang Jian-yu, "Remote sensing of human body by stepped frequency continuous wave," *3rd International Conference on Bioinformatics and Biomedical Engineering*, ICBBE 2009.

[23] A.S. Bugaev, V.Y.Chapursky, S.I.Ivashov, "Through Wall Sensing of Human breathing and heart beating by Monochromatic Radar" *Tenth International Conference on ground penetrating radar,* Delft, The Netherlands, pages 291-294, June 21-24, 2004.

[24] Bassem R Mahafza, "Radar Systems Analysis and Design using MATLAB" © 2000 by Chapman anh Halll CRC, ISBN 1-58488-18.

[25] S. Jefrernov, B. Levitas, "On application of a pulse method in detectinga living object" *12th International conference on Microwaves and Radar,* MIKON 1998, vol., pages 765 - 768.

[26] M. Jelen and E. M. Biebl, "Multi-frequency sensor for remote measurement of breath and heartbeat" Advances in Radio Sci., 4, 79-83, 2006

[27] Nicolas Petrochilos, Meriam Rezk, Anders Host-Madsen, VictorLubecke, and Olga Boric-Lubecke, "Blind separation of human heartbeats and breathingby the use of a Doppler radar remote sensing," *IEEE International conference on Acoustics, Speech and Signal Processing,* ICASSP 2007, vol I, pages 1-333 - 1-336.

[28] Soldovieri, F. and Solimene, R., 2007, "Through-wall imaging via a linear inverse scattering algorithm" *IEEE Geoscience and Remote Sensing Letters*, 4, pp. 513–517.

[29] Ahmad, F., Amin, M. G. and Kassam, S. A., 2005, "Synthetic aperture beamformer for imaging through a dielectric wall" *IEEE Transactions on Aerospace and Electronic Systems*, 41, pp. 271–283.

[30] A.M. Attiya, A. Bayram, A. Safaai-Jazi and S.M. Riad, "UWB applications for through-wall detection," in *Antennas and Propagation Society International Symposium, IEEE,* vol. 3, pp. 3079 – 3082, 2004.

[31] G. Barrie, "Ultra-wideband synthetic aperture: data and image processing," Defense R&D Canada DRDC Ottawa, Tech. Memorandum, TM 2003-015, Jan. 2003.

[32] Yang, Y. and Fathy, A.E., 2005, See-through-wall imaging using ultra wideband short–pulse radar system. In *IEEE Antennas and Propagation Society International Symposium*, 3–8 Jul. 2005, Washington, DC, USA, pp. 334–337.

[33] Yoon, Y. S. and Amin, M.G., 2009, Spatial filtering for wall-clutter mitigation in through the wall radar imaging. *IEEE Transactions on Geoscience and Remote Sensing*, 47, pp. 3192–3208.

[34] Gaikwad A.N.; "Study of through wall imaging for target detection" *PhD Thesis, Deptt of Electronics and Computer*, IIT Roorkee, June 2011.

[35] C. Debes , J. Hahn, A,M. Zoubir and M.G. Amin, "Feature Extraction in Through-Wall Radar Imaging," In *IEEE Intl. Conference on Acoustics, Speech and Signal Processing,* pp.3562-3565, 2010.

[36] Akduman, I., Crocco, L. and Soldovieri, F., 2010, Experimental validation of a simple system for through-the-wall inverse scattering. *IEEE Geoscience and Remote Sensing Letters*, 99, pp. 258–262

[37] D. D. Ferris Jr. and N. C. Currie, "Microwave and millimeter wave systems for wall penetration," In *Proceedings of SPIE*, vol. 3375, pp. 269-279, 1998.

[38] Chaturvedi P.; "Study of through wall imaging for target detection" *M. Tech Dissertation, Deptt of Electronics and Computer*, IIT Roorkee, June 2011.

[39] S. Jefrernov, B. Levitas, "On application of a pulse method in detecting a living object" *12th International conference on Microwaves and Radar,* MIKON 1998,vol. ,pages 765 - 768.

[40] Waymond R. Scott, Jr., James S. Martin, "Experimental investigation of the acousto-electromagnetic sensor for locating land mines" *In Proceedings of SPIE*, Vol. 3710, April 1999.

[41] S.I. Ivashov et al. "Detection of Human Breathing and Heartbeat by Remote Radar" *Progress in Electromagnetic Research Symposium* 2004, Pisa, Italy, March 28 – 31.

[42] Hong Wang, Ram M. Narayanan, and Zheng Ou Zhou "Through-Wall Imaging of Moving Targets Using UWB Random Noise Radar" *IEEE Antennas and Wireless Propagation letters*, VOL. 8, 2009

[43] Nag, S.; Fluhler, H.; Barnes, M.; "Preliminary interferometric images of moving targets obtained using a time-modulated ultra-wide band through-wall penetration radar," *Radar Conference, 2001. Proceedings of the 2001 IEEE*, vol., no., pp.64-69, 2001.

[44] Nicolaescu, I. and Genderen, P.V., 2008, Archimedean spiral antenna calibration procedures to increase the downrange resolution of a SFCW radar. *International Journal of Antennas and Propagation*, 2008, pp. 1–7.

[45] Ahmad, F., Amin, M. G. and Mandapati, G., 2007, Auto focusing of through the wall radar imagery under unknown wall characteristics. *IEEE Transaction Image Processing*, 16, pp. 1785–1795.

[46] C.H. Gierull; "Bistatic Synthetic Aperture Radar" Technical Report, DRDC Ottawa TR 2004-190 ; November 2004

[47] Li Xin; Huang Xiao-tao; Fan Chong-yi; Liu Wen-yan; Peng Shi-rui; , "System characteristics of UWB Bistatic through-wall SAR," *Radar (Radar), 2011 IEEE CIE International Conference on* , vol.1, no., pp.924-928, 24-27 Oct. 2011